REPUBLIQUE ALGERIENNE DEMOCRATIQUE ET POPULAIRE

MINISTERE DE L'ENSEIGNEMENT SUPERIEUR ET DE LA RECHERCHE SCIENTIFIQUE

ECOLE NATIONALE SUPERIEURE DE LAGHOUAT

DEPARTEMENT : MATHEMATIQUES

MEMOIRE DE MAGISTER

En vue de l'obtention du diplôme de Magister en Physique

Option : Interaction champ-matiére

THEME DU PROJET :

Thickness measurement of thick metallic plates by an eddy current multi-sensor system

Présenté par **:**

Mr. Nebair Hocine

Dirigé par :

Pr. Cheriet Ahmed

Dr. Helifa Bachir

DEVANT LES MEMBRES DU JURY

Mr. LEFKAIER Ibn Khaldoun	Professeur	Université de Laghouat	Président
Mr. BENTRIA Bachir	Professeur	Université de Laghouat	Examinateur
Mr. HAMIMID Mourad	MCA	Univ de Bordj Bou Arreridj	Examinateur
Mr. CHERIET Ahmed	Professeur	Université de Biskra	Directeur de mémoire
Mr. HELIFA Bachir	MCA	Université de Laghouat	Co- Directeur
Mr. ALAOUI Abdelkrim	MCB	E.N.S de Laghouat	Invité

ANNÉE UNIVERSITAIRE : 2016-2017

Acknowledgment

This work was conducted jointly in the team Non Destructive Characterization of Materials **NDTM** of the Laboratory of Materials Physics **LMP** of Laghouat University and in the Laboratory of Electrical Engineering of the Biskra University **LGEB**.

First of all, I would like to especially thank Mr. **Ibn Khaldoun LEFKAIER**, Professor at the Laghouat University, Director of the **LMP** laboratory and responsible of our magister formation: Field-Matter Interaction at the Higher Normal School of Laghouat for the confidence he makes it welcoming me as a magister student in the **LMP** laboratory, and for his valuable helpers.

I would like to express my sincere thanks and my deep gratitude to the director of this brief, Mr. **Ahmed CHERIET**, Professor at the University of Biskra, for his confidence, generosity, and patience, that helped me to overcome the most delicate moments of this brief.

I would like to express my gratitude and deep gratitude to my co-director of this brief, Mr. **Bachir HELIFA**, Lecturer 'A' at the University of Laghouat, for his support during difficult times and for his constant optimism and enthusiasm. Working with him was a great satisfaction.

I want to express my appreciation and deep gratitude to Mr. **Mohamed YOUSFI**, Professor at the University of Laghouat and the former director of the Higher Normal School of Laghouat having opened this magisterial session.

I would like to express my sincere thanks to the members of the jury:

I would like to thank again Mr. **Ibn Khaldoun LEFKAIER**, Professor at the University of Laghouat, and Director of the Materials Physics Laboratory, for honoring me to chair the jury of this brief.

I express my sincere and deep gratitude to Mr. **Bachir BENTRIA**, Professor at the Laghouat University, who has done me the honor of accepting to review and evaluate this work

Mr. **Mourad HAMIMID**, Senior Lecturer, 'A' at the University of Bordj Bou Arreridj, who did me the honor to accept to review and evaluate my work.

Mr. **Abdelkrim ALAOUI**, Lecturer, class 'B' at ENS Laghouat, who did me the honor to accept my invitation.

I would like to thank Mr. **El Ghoul Islam Nacereddine**, for providing me with helpful suggestions throughout this work and for his wise advice on how to do my work.

I would like to thank Mr. **Abdelkader BELAKDAR**, Deputy Director in charge of pos-graduation and research at ENS Laghouat for the facilities he showed us during this magister.

I would like to thank especially to my **dear parents**, who have always believed in me and gave me help and comfort, my brothers and my sisters to express my deep gratitude for their support.

Finally, I would like to thank all the members of the **LMP** laboratories of Laghouat University, and **LGEB** Laboratory of Biskra University.

Table of contents

Chapter II : Modeling of Eddy Current Nondestructive Evaluation (EC-NDE)

Chapter III : Application: Thickness evaluation of thick aluminum plates

List of figures

List of tables

GENERAL INTRODUCTION

General Introduction

In industrial sector, nondestructive evaluation NDE aimed at controlling without damaging the parts in question represents an important phase in the maintenance and monitoring of industrial installations in order to avoid any damage that may occur as a result of a failure. As a result, the task nondestructive evaluation NDE has become an industrial necessity in the aeronautical and nuclear fields...etc. The consequences of a failure are often expressed in terms of personal or environmental safety. For example, in a nuclear reactor, the fuel cladding is a decisive element for the safety of the installation. Indeed, most incidents in such installations are due to the cracking of these sheaths [HUR 06, HUR 10, HEL 06, HEL 12, ZAI 12, ZOR 12]. The speed and reliability of the evaluation technique employed are crucial in order to reduce the maintenance cost and optimize the service life of the installations.

The techniques used in NDE are diverse; visual inspection, liquid penetrant, magnetic testing, ultrasonic testing, radiographic testing, thermography inspection, eddy currents EC ... etc. The nondestructive evaluation by eddy current (NDE-EC) is widely used. It is very present in the field of aeronautics [HEL 12]. Indeed, the NDE-EC is a very sensitive technique for defects of geometrical nature such as cracks, thickness measurement...etc. In addition, it is robust and less expensive compared to the methods mentioned.

The development of NDE-EC processes became possible due to numerical modeling of electromagnetic systems. This modeling also helps to understand the electrical and magnetic phenomena involved. Several research studies have focused on the modeling and simulation of the NDE-EC. Knowing that this modeling is often associated with an inversion problem in order to characterize the physical and geometrical properties of the part [CHE 07, HEL12, BEN 06]. The NDE-EC has taken a large place in various nondestructive evaluations such as:

- Measurement of the geometrical dimensions of the pieces (thickness ... etc.),
- Defect detection,
- Electromagnetic characterization of materials (electrical conductivity ... etc).

In the field of nondestructive testing and evaluation of product, there is an enormous demand for accurate measurement of metallic plate thickness [PIN 14]. Thick metallic plates are usually controlled by using capacitive effect based sensors or ultrasound techniques and using laser triangulation [GOM 10, PET 12, DON 10]. The ultrasound sensor requires a coupling liquid which makes the method appear slowly and costly, while the capacitive one seems very sensitive to noise. When applicable the eddy current nondestructive evaluation method (EC-NDE), which making use of electromagnetic induction, offers several advantages such as being easy to implement and contactless. In addition, electrical signals provided from the eddy current sensors can be analyzed as the inspection progresses, and hence allows

automation control in real time. The EC-NDE can be regards as a characterization technique that finds its application in the maintenance of process and in some industrial applications which require high surveillance. Nevertheless, this method is limited for thin metallic plates with respect to the skin effect phenomenon.

The principal objective of our work is to propose an alternative method for thickness measurement of thick metallic plates based on bi-eddy current sensor (two eddy current sensors).

This work is divided into three chapters, the first chapter presents the basics needed to study the different methods of nondestructive evaluation NDE used in the industrial domain also the different types of eddy current sensors used. In the second chapter we present the mathematical equations and formulations governing electromagnetic systems as well as the resolution of these equations by the finite volume method FVM, also we will present to a field calculation by the finite volume method FVM for to calculate the impedance variations of two eddy current sensors. The third chapter concerns the practical realization of a test bench dedicated to the experimental thickness measurements of thick aluminum plates.

Chapter I
General Nondestructive Evaluation by Eddy Current (NDE -EC)

I.1 Introduction

Nondestructive techniques (NDT) are used widely in the metal industry in order to control the materials quality, the terms nondestructive evaluation (NDE) is also commonly used to describe this technology; it can operate in a production line, in a facility under operation, and in maintenance time. This diversity is due to a technical number of features including speed, high sensitivity, and the possibility of its performance on complex structures with adaptable sensors [CHE 09,BAC 09, MHE 07].

Considered in this ability to look for the proper functioning, the definition of NDE assumes knowledge of all the phenomena involved, especially the harmfulness of defects or evaluation of thicknesses, their evolution over time, and the general mechanics laws in practice. Nondestructive control specialists are confronted with interpretation problems of control results compared to criteria established in conjunction with the plate designer.

In this chapter, we present nondestructive evaluation techniques and especially those using eddy currents, we will also present the different inductive sensors and eddy current sensors, sensor layout, different excitation modes and an impedance of the sensor. Finally, we will present some measurement methods thick thickness.

I.2 Nondestructive evaluation techniques

Nondestructive evaluation (NDE) is a wide group of:

I.2.1 Visual Inspection

Visual Inspection is the predominant nondestructive evaluation technique used in inspections in the past. Tools include magnifying glasses and mirrors, it used in maintenance of material such as flat products of sheet types, glass…etc. [DUM 96, PAU 05].

- Advantages
  - ✓ Simple, fast and inexpensive examination;
  - ✓ Flexibility of inspection.

- Disadvantages
  - ✓ Detection limited to superficial defects;
  - ✓ The surface must be clean.

I.2.2 Liquid Penetrant

Liquid penetrant is one of the ancient and easy nondestructive evaluation (NDE) methods in the industry, where its earliest versions date back to the 19th century. This method is used for detecting discontinuities open to the surface. The penetrant may be applied to all non-ferrous materials and ferrous materials, there are four basic steps to follow when using the penetrant method (Fig I.1): Pre-cleaning part after that Apply penetrant, a waiting period to insure the dye has penetrated into the narrowest cracks, the excess penetrant is cleaned from the surface of the sample then apply developer, by visual inspection under white or ultraviolet light, fluorescent dye are identified and located, that way defining the defect [DUM 96, , PAU 05, CHO 09, MOH 07].

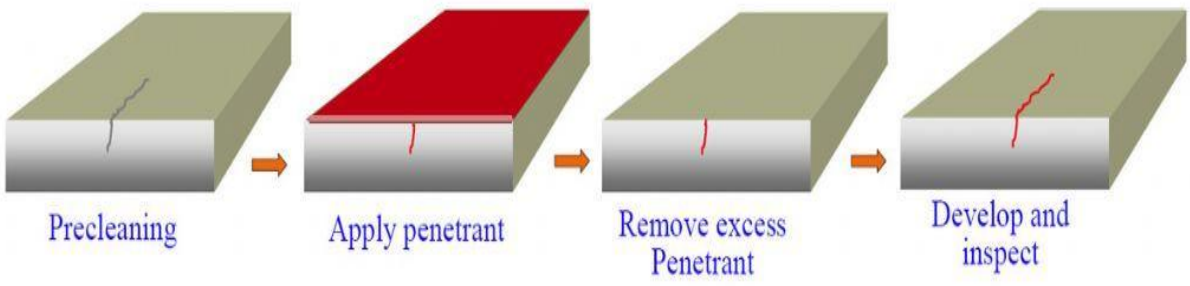

Fig I.1 Penetrant Inspection

- Advantages
  - ✓ High sensitivity to small surface discontinuities;
  - ✓ Easy inspection of parts with complex shapes;
  - ✓ It is easy and requires minimal amount of training;
  - ✓ Applied to dielectric and non-ferromagnetic materials.

- Disadvantages
  - ✓ Detects flaws only open to the surface;
  - ✓ Materials with porous surfaces cannot be examined using this process;
  - ✓ Examiner must have direct access to surface being examined;
  - ✓ Multiple process steps must be performed and controlled.

I.2.3 Magnetic testing

Magnetic testing is a family of nondestructive evaluation (NDE) technique for crack identification that relies on local or complete magnetization of the component. The idea of using magnetic techniques for nondestructive evaluation of ferromagnetic materials originated in 1905. It is used to examine ferromagnetic materials for defects that result in a transition in the magnetic permeability of a material. It can detect surface and near surface defects, where it is detected as follows: a magnetic field is established in a component made from

ferromagnetic material. The magnetic lines of force travel through the material and exit and reenter the material at the poles. Defects such as cracks or voids cannot support as much flux, and force some of the flux outside of the part. Magnetic particles distributed over the component will be attracted to areas of flux leakage and produce a visible indication (Fig I.2) [DUM 96, BEN 06].

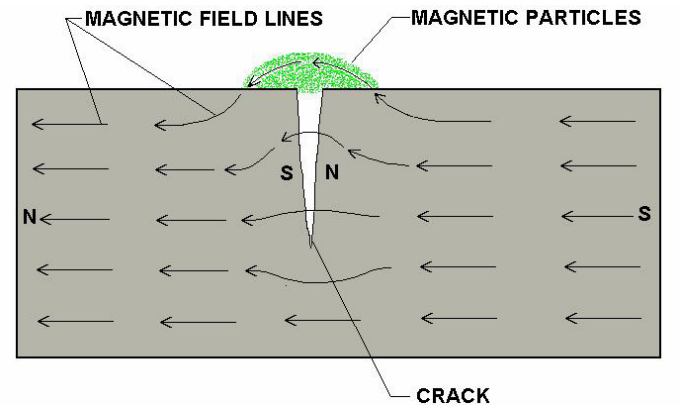

Fig I.2 Inspection by Magnetic testing

- Advantages
  - ✓ Equipment costs are relatively low;
  - ✓ Large surface areas of complex parts can be inspected rapidly;
  - ✓ Can detect surface and subsurface flaws;
  - ✓ Surface preparation is less critical than it is in penetrant inspection.

- Disadvantages
  - ✓ Requires relatively smooth surface;
  - ✓ Paint or other nonmagnetic coverings adversely affect sensitivity;
  - ✓ Large currents are needed for very large parts;
  - ✓ Demagnetization and post cleaning is usually necessary.

I.2.4 Ultrasonic testing

Ultrasonic testing (UT) is a nondestructive evaluation techniques based on the propagation of ultrasonic waves in the material tested; Ultrasonic evaluation is used to measure the thickness of thick materials and can be used for flaw detection such as crack (Fig I.3), dimensional measurements, etc. A typical UT system consists of several functional units, such as the pulser/receiver, transducer and display devices. The operation is done as follows: High frequency sound waves are introduced into a material and they are reflected back from surfaces or flaws, reflected sound energy is displayed versus time, and inspector can visualize a cross section of the specimen showing the depth of features that reflect sound [AUL 10, CRU 15, LUB 15, JAC 96, MAR 11].

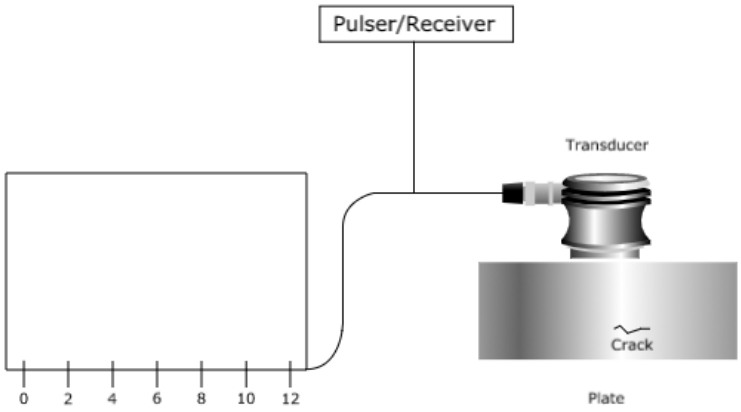

Fig I.3 Principles of ultrasonic testing

- Advantages
  - ✓ It is sensitive to both surface and subsurface discontinuities;
  - ✓ Only single sided access is required;
  - ✓ Real-time inspection and detection;
  - ✓ Minimal part preparation is required;
  - ✓ Provides distance information;
  - ✓ Electronic equipment provides immediate results.

- Disadvantages
  - ✓ Surface must be accessible to probe and coupling;
  - ✓ Reference standards are often needed;
  - ✓ Linear defects oriented parallel to the sound beam may go undetected;
  - ✓ Technique often very expensive ;
  - ✓ Sensitive to the nature and orientation of defects.

I.2.5 Radiographic testing

Radiographic testing is a method of nondestructive evaluation, is used in a very wide range of applications including medicine, engineering and security, etc. The X-ray or Gamma-ray radiographic testing methods are often used for detecting weld defects as a nondestructive evaluation method, The radiation used in radiography testing is a higher energy version of the electromagnetic waves that we see as visible light, used to inspect almost any material for surface and subsurface defects, Radiography may be performed prior or afterheat treatment and in rough, the object of this method is placed between the radiation source and detector. The thickness and the density of the material that X-rays (or Gamma-ray) must penetrate affect the amount of radiation reaching the detector. This variation in radiation produces an image on the detector that often shows internal characteristics of the material under test (Fig I. 4) [HOL 98, MAI 04].

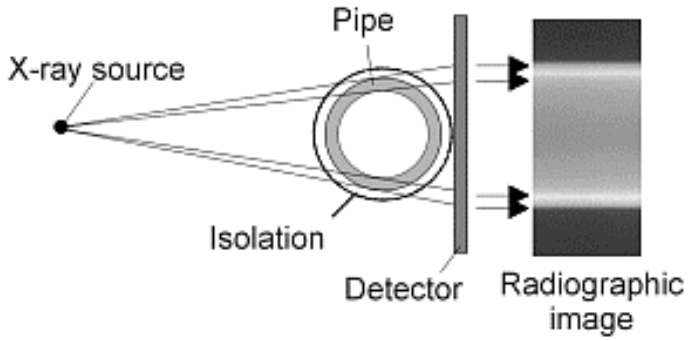

Fig I.4 Principles of radiographic testing

- Advantages
  - ✓ Can be used to inspect virtually all materials;
  - ✓ Detects surface and subsurface defects;
  - ✓ Ability to inspect complex shapes;
  - ✓ Minimum part preparation is required;
  - ✓ Easy to Transport (X-ray generators of low energies, radioactive devices Portable);
  - ✓ Appreciate the nature and size of defects.

- Disadvantages
  - ✓ This technique is extremely costly and imposes safety requirements;
  - ✓ Access to both sides of the structure is usually required;
  - ✓ Orientation of the radiation beam to non-volumetric defects is critical;
  - ✓ Field inspection of thick part can be time consuming;
  - ✓ Relatively expensive equipment investment is required;
  - ✓ Possible radiation hazard for personnel;
  - ✓ The interpretation of the images requires a level of expertise of the operator;
  - ✓ The risk of not detecting the cracks occurring along the axis of the beam.

I.2.6 Thermography inspection

Thermography inspection is a family of nondestructive evaluation of parts, uses a camera have great numbers of sensors which can reveal and evaluate small temperature differences, showing these differences displayed on a computer in the form of an image (Fig I.5); there are two basic types of thermography; passive thermography and active thermography. In both cases, the investigation consists of detecting the presence of a temperature gradient that reveals the presence of a defect, a gradient that can be caused either by a rise or a fall in temperature [PAU 05].

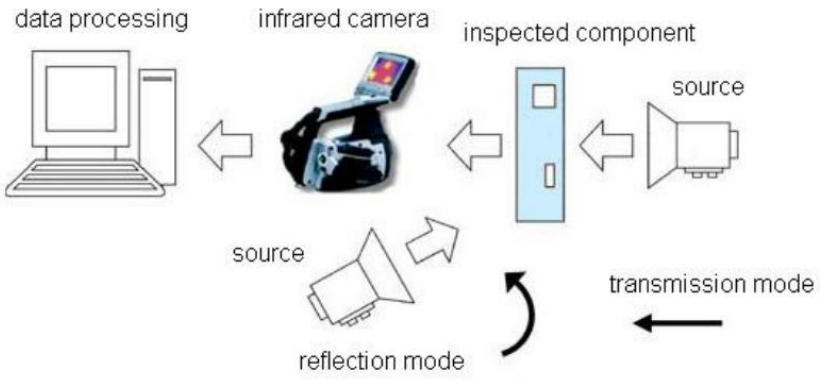

Fig I.5 Thermography inspection

- Advantages
  - ✓ contactless method;
  - ✓ The entire thickness of the room is generally controlled;
  - ✓ The cavities (air bubble fields, cracks,...) are well detected;
  - ✓ Sensitivity to the detection of small defects;
  - ✓ The archiving of the results is guaranteed using the infrared camera.

- Disadvantages
  - ✓ Measurement difficulties related to disruptive effects;
  - ✓ Difficulties in locating the depth of the defects, because the image obtained gives a projection of the latter on the plane of the test piece;
  - ✓ The interpretation of measurements is not always easy, especially to identify the nature of the defects;
  - ✓ The interpretation phase of the results presents some restrictions for a total automation of the technique.

I.3 Eddy current method

The eddy current method is the most used method of electromagnetic evaluation of electrically conductive materials (thickness measurement, defect detection etc.)[ELG 15, HEL 06, HUR 06, HUR 10, HON 15] at very high speeds that does not require any contact between the test piece (ex: conductive plate) and the sensor, also it used in nuclear, power, petrochemical, automotive, aircraft and engineering industry. However, this method is only usable on metallic media to evaluate thicknesses or defects at small depths [DUM 96, ABD 98, MAA 94]

- Advantages
  - ✓ Test probe does not need to contact the part;
  - ✓ Simple, inexpensive and fast;

- ✓ Method can be used for more than flaw detection (thickness evaluation);
- ✓ Efficiency of the technique despite the complexity of the electromagnetic phenomena implemented;
- ✓ Automation possible for parts of constant geometry (tubes, bars, ribbons and cables);
- ✓ Minimum part preparation is required;
- ✓ No safety conditions for the operator or the environment.

➢ Disadvantages

- ✓ Only conductive materials can be inspected;
- ✓ Ferromagnetic materials require special treatment to address magnetic permeability;
- ✓ Depth of penetration is limited;
- ✓ Flaws that lie parallel to the inspection probe coil winding direction can go undetected;
- ✓ Skill and training required is more extensive than other techniques;
- ✓ Surface finish and roughness may interfere;
- ✓ Reference standards are needed for setup.

I.3.1 Principle of eddy current

A sensor of copper wire is the rife method of inducing eddy currents, Alternating electrical current is passed through a sensor producing a magnetic field, when a single alternating energized EC-sensor placed above an electrically conductive plate, and an alternating magnetic field penetrates the plate and generates eddy currents (Fig I.6). The value of the magnetic field depends on several factors including the following: Geometry of the sensor, geometry of the plate, current and frequency in the sensor, electrical conductivity σ and magnetic permeability μ of the sensor [BLI 97].

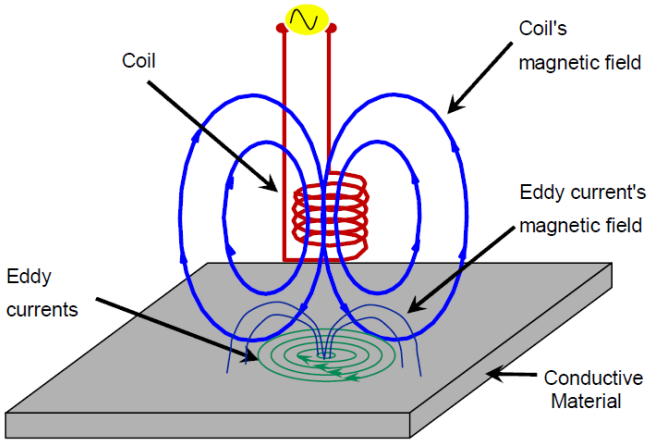

Fig I.6 Principle of eddy currents

1.4 Depth of penetration

The great part of eddy currents flows in the so-called depth of penetration δ, The depth of penetration into a material is affected by the frequency of the excitation current and the electrical conductivity and magnetic permeability of the conductive plate, which is given by the following equation:

$$\delta = \frac{1}{\sqrt{\pi f \mu \sigma}} \tag{I.1}$$

δ: Depth of penetration (m).

f : The frequency of the source current (Hz).

μ : Magnetic permeability of the conductive plate.

σ : Electrical conductivity of the conductive plate (S/m).

The depth of penetration decreases with increasing frequency and increasing conductivity and magnetic permeability (Fig I.7); it is defined as the depth at which the intensity of the radiation inside the material falls to 1/e (about 37%) of its original value at the surface (Fig I. 8) [GIL 88, HMG 09].

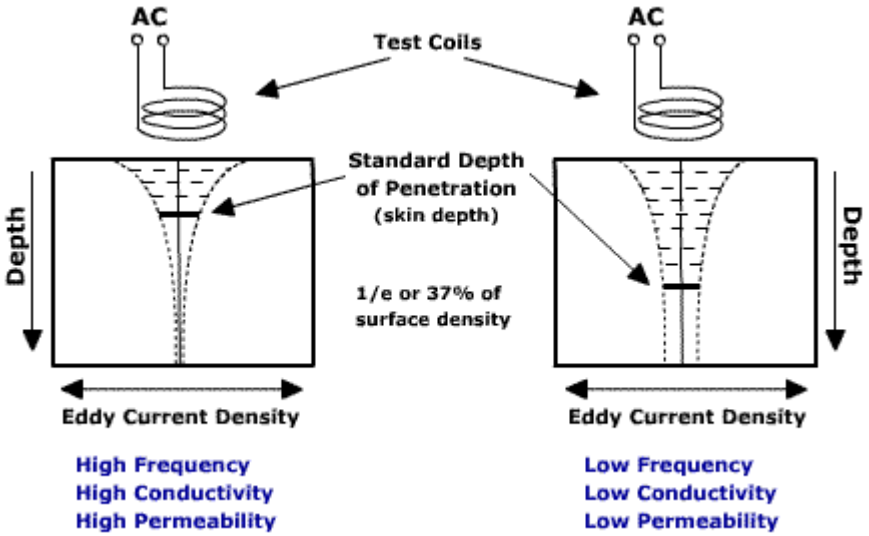

Fig I.7 Eddy current depth of penetration

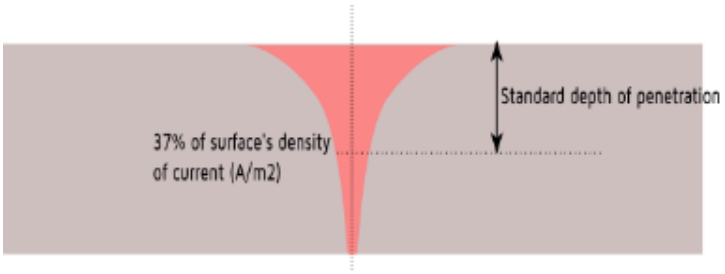

Fig I.8 Density of eddy current

1.5 Different inductive Sensors

There are many ways to implement the winding in order to realize eddy current sensors.

I.5.1 Absolute sensor

I.5.1.1 Dual function sensor

It consists of a single transmitter-receiver coil that creates the alternative flows through the current that flows and undergoes impedance variations that can be detected by measuring its output signal (Fig I.9) [BEN 06, CHO 09, GIL 88].

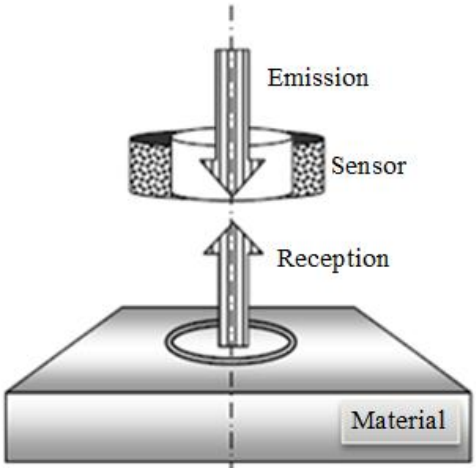

Fig I.9 Dual function sensor

I.5.1.2 Separate function sensor

Separate function sensor consists of two coils one exciter to create the flow and the other receiver to collect it. These two coils are molded in a single enclosure to avoid any accidental modification of their mutual; this type of sensor is widely used for low frequency controls (Fig I.10) [BEN 06, CHO 09, GIL 88, ZER 10, RAV 09].

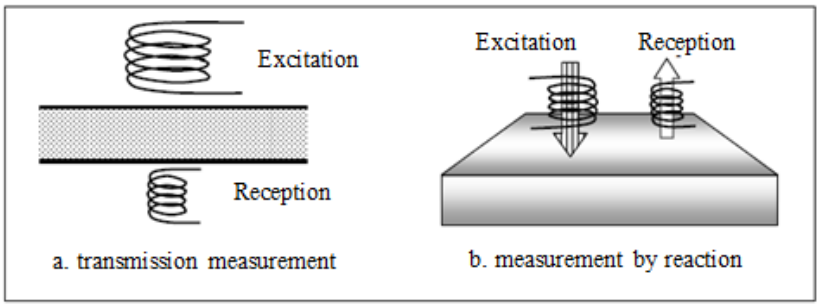

Fig I.10 Separate function sensor

I.5.2 Differential sensors

Differential sensor consists of two coils which impedance difference is measured, this coils is particularly used to detect discontinuities during its movement along a plate while avoiding induced disturbances such as variations in sensor-plate distance (Liftoff) (Fig I.11)[DUM 96, BEN 06, BUR 04, LAK 10].

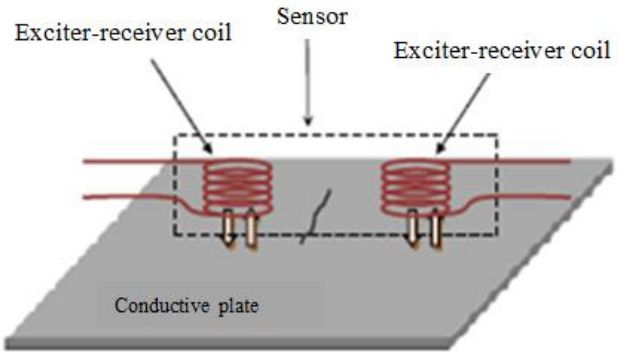

Fig I.11 Differential sensor

I.5.3 Phased array sensor

It is a sensor made by assembling a set of identical coils arranged in matrix form that function in an autonomous manner (Fig I.12) [ABD 06, OUK 97, RAV 09, ZAO 09].

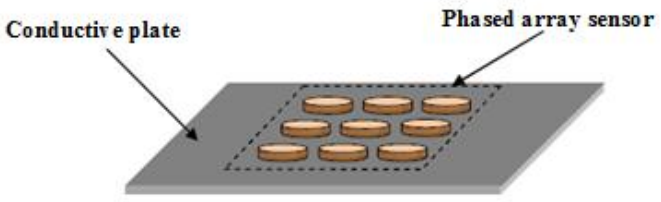

Fig I.12 Phased array sensor

I.6 Eddy current sensors

I.6.1 Different coils geometries

There are several configurations of the excitation coil related to the conductive plate (Fig I. 13), we will cite three important. The internal coils (Fig I.13.a), the encircling coils (Fig I. 13.b) and the simple or flat coils (Fig 13.c and Fig I.13.d) [BEN 06, OUK 97].

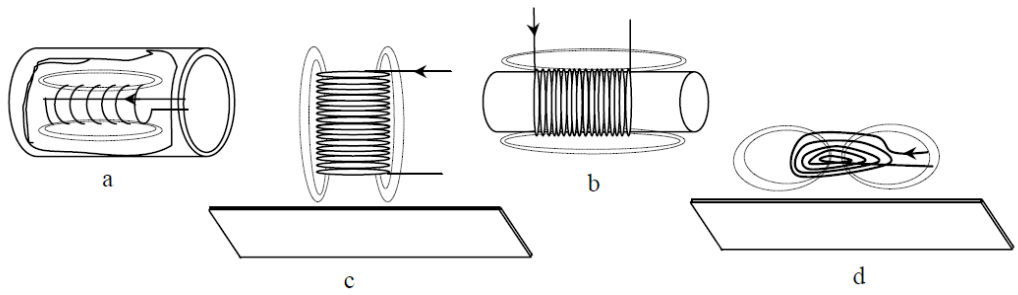

Fig I.13 Different coils geometries,

(a) internal coil, (b) encircling coil, (c) simple coil, (d) flat coil

I.6.2 Different magnetic circuit geometries

This can be made of low-frequency laminated plates or ferrite for high frequencies. Its role is to channel the magnetic field lines to the space zone where the conductive plate will be placed for to inspect (Fig I.14) [BEN 06, OUK 97].

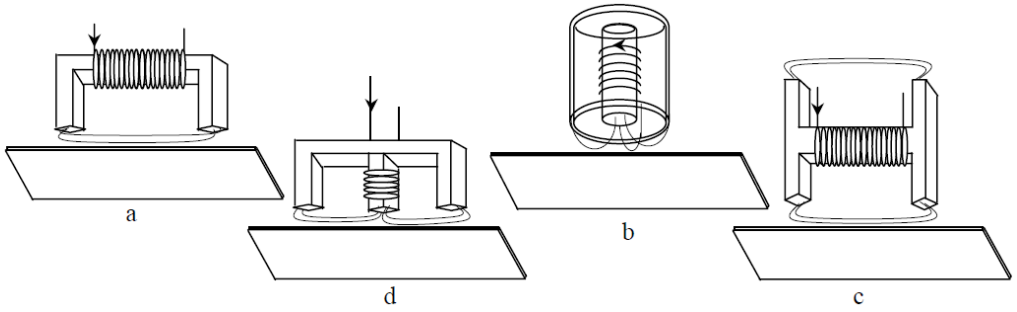

Fig I.14 Different magnetic circuit geometries,

(a) U coil, (b) Potted coil, (c) H coil, (d) E coil

I.7 Sensor layout

In practice, there are essentially three layouts [DUM 96, BEN 06, OUK 97]:

I.7.1 First layout: encircling sensors

This layout is intended for control of long products of simple shape and modest diameter such as wires, bars and tubes (Fig I.15).

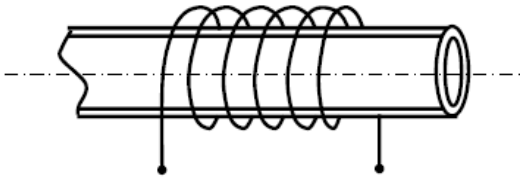

Fig I.15 Encircling sensors

I.7.2 Second layout: internal sensors

This sensor is dedicated to control the tubes from the inside, for which the coils are also molded concentrically to the axis of the product (Fig I.16).

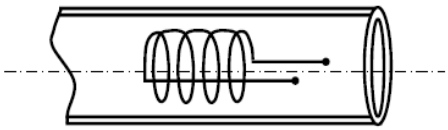

Fig I.16 Internal sensor

I.7.3 Third layout: point sensors

This layout is adapted to the occasional explorations in manual control or the sweeping of big surfaces in automatic control (Fig I.17).

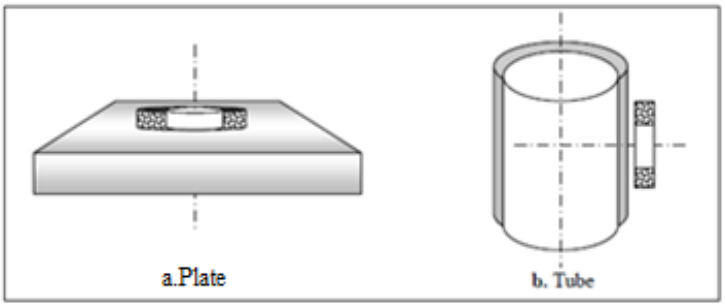

Fig I.17 Point sensors

I.8 Different excitation modes

There are three excitation modes:

- ✓ Mono-frequency excitation.
- ✓ Multi-frequency excitation.
- ✓ Pulse excitation.

I.8.1 Mono-frequency excitation

The Mono-frequency is used in nondestructive evaluation by eddy current (EC-NDE). The induced currents are obtained by a sinusoidal excitation of fixed frequency. The choice of the frequency depends essentially on the intended application and the sensitivity of the desired parameters. However, it will have to be in a reasonable range. Indeed:

- ☞ For too low a frequency, the amplitude of the induced currents will be low and the measurement accuracy insufficient because of the noise.
- ☞ Too high a frequency causes parasitic capacitive phenomena, generated in particular by the inter-coil capacitances of the sensor [BEN 06].

I.8.2 Multi-frequency excitation

The multifrequency method has been widely used in nondestructive evaluation by eddy current (EC-NDE), Embodiments of multi-frequency excitation are described. In various embodiments, a natural frequency of a device may be determined. Using the methods of multi- frequency excitation, new operating frequencies, operating frequency ranges, resonance frequencies, resonance frequency ranges, and/or resonance responses can be achieved for devices and systems. Also this technique is widely used for the inversion of data provided by the sensor to determine the parameters of a target despite the presence of disturbance quantities [AKN 01, OUK 97, BER 98].

The multifrequency excitation can be realized either:

- ☞ In sequence: The disadvantage of this method lies in the significant acquisition time which slows the measurement.
- ☞ Simultaneously: this method requires a complicated measuring device is expensive. In practice, the number of frequencies rarely exceeds four because of the complexity and difficulty of setting such devices.

I.8.3 Pulse excitation

This method represents an alternative to multifrequency excitation; it consists in emitting a broadband magnetic field by exciting the sensor with a pulse signal. The shape of the supply

signals can be: rectangular, triangular or semi-sinusoidal, the latter being the most used because of its simplicity of implementation [BOU 96, WAI 56].

I.9 Normalized impedance

Material inspection consists of measuring the impedance variations of the sensor. The object is to measure the difference between the impedance Z of the sensor with conductive plate and the impedance Z_0 (without plate). The impedance Z_0 of the sensor is:

$$Z_0 = R_0 + jX_0 \tag{I. 2}$$

R_0 and X_0 are respectively the resistance and the reactance of the sensor without plate.

The impedance Z with the plate is:

$$Z = R + jX \tag{I. 3}$$

The resistive component (R) which includes the current losses due to field penetration in the plate and the internal losses of the excitation sensor and the reactive term (X) represents the reactance of the excitation sensor.

To eliminate the components of the vacuum impedance R_0 and X_0 (inductance of the sensor) and keep only the geometry of the sensor, its position to the material (Liftoff) and the geometric and physical characteristics of the sensor, geometric of the plate (Fig I.18) and the impedance of the sensor is normalized in the presence of the material. This normalization is given by:

$$Z_n = R_n + jX_n = \frac{Z - R_0}{X_0} \tag{I. 4}$$

$$R_n = \frac{R - R_0}{X_0} \quad \text{and} \quad X_n = \frac{X}{X_0} \tag{I. 5}$$

R_n and X_n are respectively the normalized resistance and reactance of the sensor.

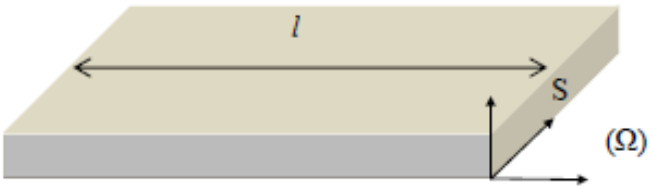

Fig I.18 Plate Geometry

I.10 Measurement methods of thick thickness

Several thicknesses have been the subject of many research papers such as "Air-coupled Thickness Measurements of Stainless Steel" using ultrasonic transmitted and receiver placed on 100 mm on each side of the plate, this plate consists of three areas, A, B and C, with thickness 10 mm, 9.8 mm and 9.6 mm respectively, and a transparent box was placed on top of the setup to minimize the convection of the air between the transducers and the steel plate (Fig I.19).

Sending and receiving pulses (with frequencies from 200 to 600 kHz were used), the Rx receives the pulses sent by Tx with Rx was connected to a preamplifier. Measurements were done in each of the three regions by manually moving the transducers parallel to the steel plate [PET 12].

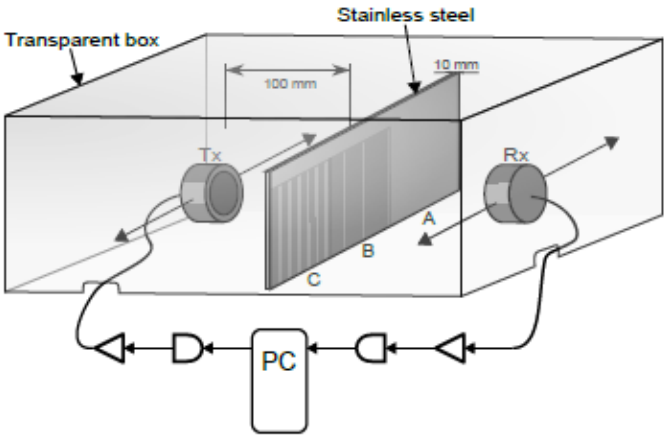

Fig I.19 Regions A, B, and the distance from the transducers to target [PET 12]

Wuliang Yin [YIN 08] made a research on the thickness measurement of metallic plates with an electromagnetic sensor using phase signature analysis this research observed deferent thickness measurements, thick and thin plates, in the section I, he introduced the methods and used in this research work. The section II the author listed and explained to obtain plot thickness measurements. As a result, this research found out a small portable measuring instrument that is capable of providing real-time thickness for metallic plates.

The method of obtaining thickness of the plate is bringing a plate nonmagnetic and under a coil (e the thickness of the plat, Liftoff the distance enter the plate and the coil) (Fig I.20) first we should take the phase signatures from measurements. Second, compare the phase signature with the closest match we got already.

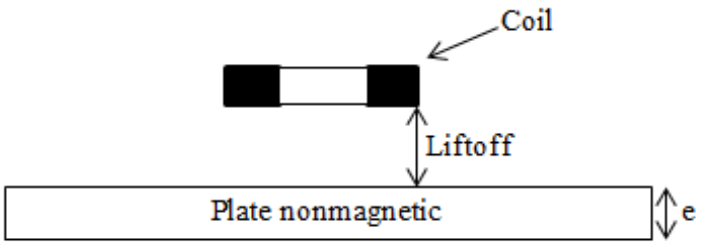

Fig I.20 Schematic of the model

Kral [KRA 11] proposed method to estimate the thickness of a conductive plate using transient eddy currents with two different probes (Fig I.21) In this work the plate used in the experiment are aluminum alloy with different thickness (1 to 4.5 mm), the method requires to be calibrated for each particular material before measuring, this measurement was used giant magnetoresistive sensor (GMRs).

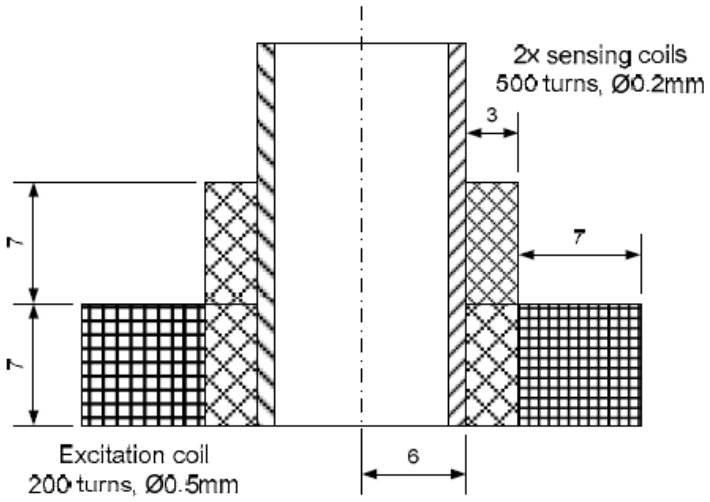

Fig I.21 Transient eddy currents with two different probes [KRA 11]

Young [YOU 08] used a differential send-receive type sensing coils composed of two coils (Fig I.22) placed in the top and the bottom of the exciting coil wound in opposite directions and connected in a series to eliminates the voltage induced by the direct field in a pulsed eddy current probe, to measure different the thicknesses from 1mm to 25mm. A 10% variation of plate thickness.

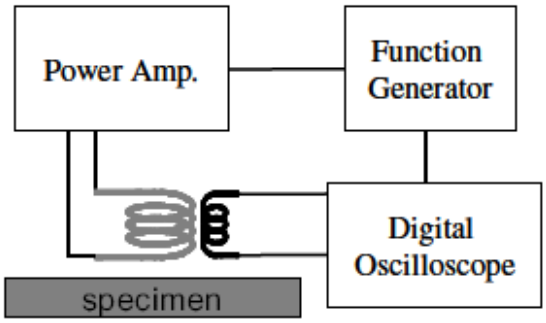

Fig I.22 Pulsed eddy current system [YOU 08]

There is method [DON 10] where the sensor measures the distance to the surface of the part independently. The thickness e is obtained by subtracting the sum of the measured values (A and B in the figure below) from the mounting distance (C in the figure below) (Fig I.23).

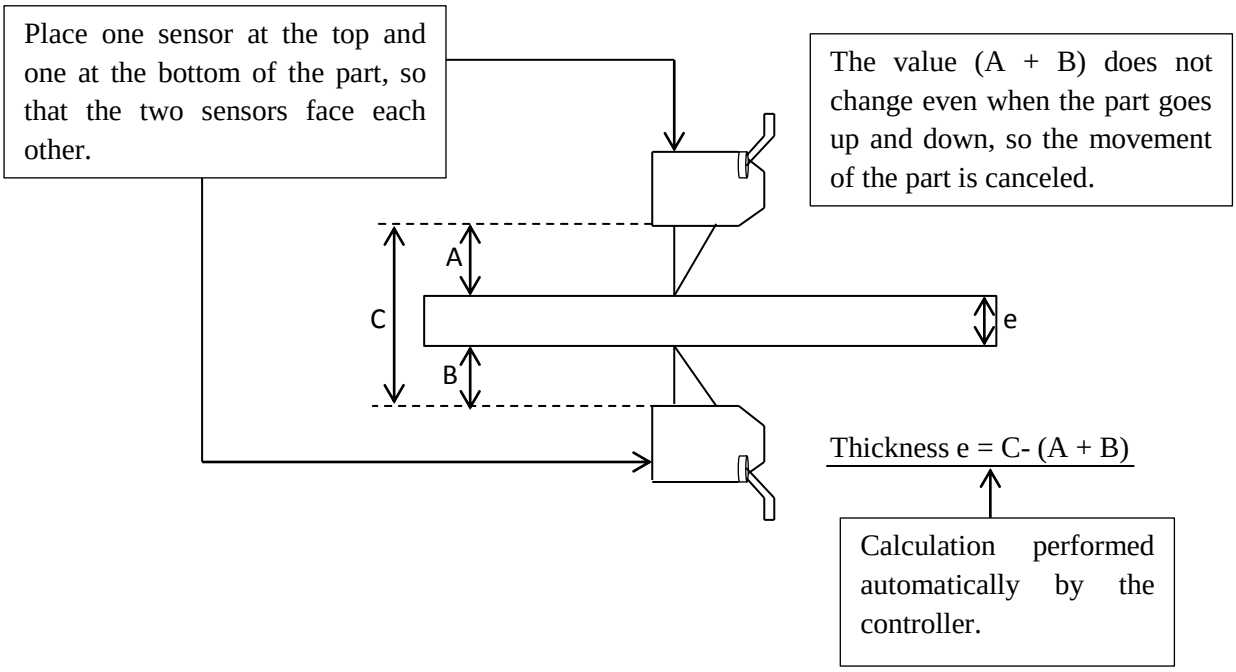

Fig I.23 Schematization of the measurement system

Measure steps, adjust the optical axes so that the two sensors are aligned, then adjust the gain so that the output voltages for the upper and lower sensors are equal to the travel from A to B of the part, and step number three enter the dimensions of the reference part in the controller. After measuring the specific thickness of the reference part, press the ZERO key on the controller to complete the adjustment.

Ribeiro [RIB 12] describes the application of the eddy current method (ECM) to measure the thickness of metallic non-ferromagnetic plates. He uses single frequency excitation and a giant magneto-resistor sensor (GMR), the experimental setup is as follows, a giant magneto-resistor is inserted along the coil axis, and the sensor voltage output is amplified by an instrumentation amplifier (Fig I.24). The method was tested experimentally with aluminum plates for thickness measurements up to 5 mm with aluminum specimens.

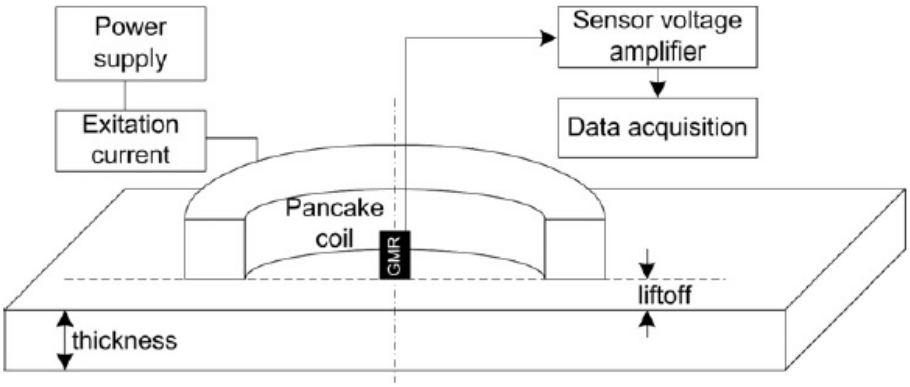

Fig I.24 Experimental setup [RIB 12]

I.11 Conclusion

In this chapter, we presented the nondestructive evaluation methods are: visual inspection, liquid penetrant, magnetic testing, ultrasonic testing, radiographic testing, thermography inspection and finally the eddy current nondestructive evaluation method (EC-NDE) which is the subject of this work. In the second part of this chapter, we reported notions on the eddy current creation and the operating principle of the different types of inductive sensors used in EC-NDE applications. Also, the main coils of these sensors are reported, described the shape and depth of penetration of the induced currents. In the second chapter, we treat resolution of electromagnetic equations by the finite volume method.

Chapter II
Modeling of Eddy Current Nondestructive Evaluation (EC-NDE)

II.1 Introduction

In the previous chapter, we presented the techniques of eddy current inspection. Actually, the inspection procedure requires a set of knowledge about the physical properties of materials on electromagnetic phenomena, as well as on inspected conductive materials. The phenomena that describe the behavior of electromagnetic devices are represented by partial differential equations (PDE). In general, the resolution of partial differential equations (PDEs) is done by analytical methods in cases of simple geometries, however these phenomena are found in geometry regions very varied, and their resolution is generally by numerical methods such as finite difference method (FDM), finite element method (FEM), finite volume method (MVF) ... etc. In this chapter we use the finite volume method. Second part of this chapter we will present to a field calculation by the finite volume method FVM for to calculate the impedance variations of two eddy current sensors.

II.2 Electromagnetism equation

The phenomena that occur in eddy current control are governed by the Maxwell's equations:

II.2.1 Maxwell's equations

Maxwell's equations, which describe the behavior of electromagnetic fields, are the basis for solving electromagnetic problems. Actually, all of electromagnetic analysis can be described by Maxwell's equations subject to given boundary conditions. It consists of:

$$\vec{rot}\,\vec{H} = \vec{J}_t \tag{II.1}$$

$$\vec{rot}\,\vec{E} = -\frac{\partial \vec{B}}{\partial t} \tag{II.2}$$

$$div\vec{B} = 0 \tag{II.3}$$

$$div\vec{D} = \rho \tag{II.4}$$

Where:

- The magnetic flux density $\vec{B}$.
- Magnetic field intensity $\vec{H}$.
- Electric flux density $\vec{D}$.
- Electric field intensity $\vec{E}$.
- Electric current density $\vec{J}_t$.
- Electric charge density ρ.

II.2.2 Constitutive relations

Constitutive relation connect $\vec{H}$ and $\vec{E}$ with $\vec{B}$ and $\vec{D}$.

$$\vec{B} = \mu \vec{H} \tag{II.5}$$

$$\vec{D} = \varepsilon \vec{E} \tag{II.6}$$

II.3 Cylindrical axisymmetric model in electromagnetism

A large part of magnetic problems can be treated in two dimensions. Recall the existence of two types of two-dimensional system: Those infinitely long powered in one direction (oz), and those with symmetry of revolution powered in the direction (o φ). In the first case (Fig II.1), the electric field $\vec{E}$ has only one component in the infinitely long direction (oz). The magnetic field $\vec{B}$ has two components along (x) and (y), thus imply a component for the magnetic vector potential $\vec{A}$ along the direction (oz).

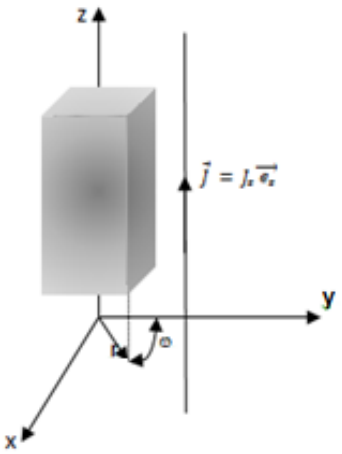

Fig II.1 Infinitely long two-dimensional system powered in direction (oz)

In the second case (Fig II.2), the current Js is directed according to the angle φ of the cylindrical coordinate system (r, φ, z), the magnetic field $\vec{B}$ has two components, one following the direction (or) and the other following the direction (oz), thus imposing for the vector potential $\vec{A}$ a single component Aφ.

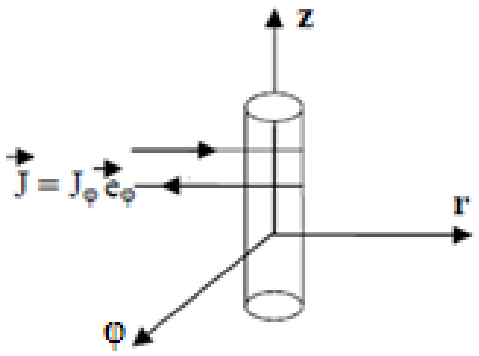

Fig II.2 Two-dimensional system with symmetry in powered direction (φ)

II.4 Magnetodynamic equation of an axisymmetric cylindrical system

For numerical calculation, different state choices variables leading to different formulations are possible. There are several formulations in electromagnetism. Among these formulations, the magnetic vector potential formulation $\vec{A}$. Based on Maxwell's equations, the equation which describes the electromagnetic phenomena which is given by the following equation:

$$\vec{rot}(\frac{1}{\mu}\vec{rot}\,\vec{A}) + \sigma\frac{\partial\vec{A}}{\partial t} = \vec{J}_s \tag{II.7}$$

The use of this formulation is very answered for the resolution of the eddy current nondestructive evaluation (EC-NDE) problems.

When the excitation current is oriented in the direction (φ) in the axisymmetric coordinates (r, z), the magnetic vector potential $\vec{A}$ has components (0, A_φ, 0). The development of equation (II.7) in the (r, z) plane which is given by the following equation:

$$\frac{\partial}{\partial z}(\frac{1}{\mu r}\frac{\partial A^*}{\partial z}) + \frac{\partial}{\partial r}(\frac{1}{\mu r}\frac{\partial A^*}{\partial r}) - \frac{\sigma}{r}\frac{\partial A^*}{\partial t} = -J_s \tag{II.8}$$

A^* is the modified magnetic vector potential ($A^* = rA_\varphi$).

This is a partial differential equation, which describes the magnetodynamic behavior of an axisymmetric device.

II.5 Different techniques resolution of Partial Differential Equations (PDE)

II.5.1 Finite difference method (FDM)

The finite difference method is one of the simplest and of the oldest methods to solve differential equations. It is based on Taylor's theorem where the differential operator is replaced by a difference operator, this method is difficult to apply to domains with complex geometry, and it is rather reserved for areas with simple geometry and regular borders such as squares and rectangles [BEL 03].

II.5.2 Finite element method (FEM)

The finite element method is more comprehensive because it is better suited to complex geometries and nonlinear materials; it can be relative easily applied for all kinds of (PDE) with various boundary conditions in nearly the same way. The finite element formulation works on a large number of discretization elements and also on different kinds of meshes within the domain. Furthermore, it also provides good results for a coarse mesh. It can easily handle complicated geometries, variable material characteristics, and different accuracy demands. It is widely used in electromagnetism although it is somewhat difficult to implement since it requires a large memory capacity and a large calculation time [KHE 06].

II.5.3 Boundary integral method (BIM)

Boundary integral equations are a classical tool for the analysis of boundary value problems for partial differential equations, when using FDM or FEM, unknown variables are calculated for the entire domain, boundary integral method attempts to use the given boundary conditions to fit boundary values into the integral equation, rather than values throughout the space defined by a partial differential equation. Once this is done, in the post-processing stage, the integral equation can then be used again to calculate numerically the solution directly at any desired point in the interior of the solution domain [LAK 11].

II.5.4 Finite volume method (FVM)

The finite volume method (FVM) is a discretization technique for partial differential equations; this method is used especially in fluid mechanics, its procedure gives a more precise solution than that provided by the FDM. This method consists in subdividing the domain of study into elementary volumes, these elements are, in the three-dimensional case, to each element of volume Dp (i = p), we associate a principal node P and six facets: e and w in the direction x, n and s in the direction y, t and b in the direction z (Fig II.3). The neighboring elementary volumes of the element Dp are represented by their main nodes: E and W along the x, N and S axis along the y, T and B axis along the z axis [CHE 07], the

partial differential equations PDE of the problem is integrated on an elementary volume [BEL 03, KHE 06, PAT 80].

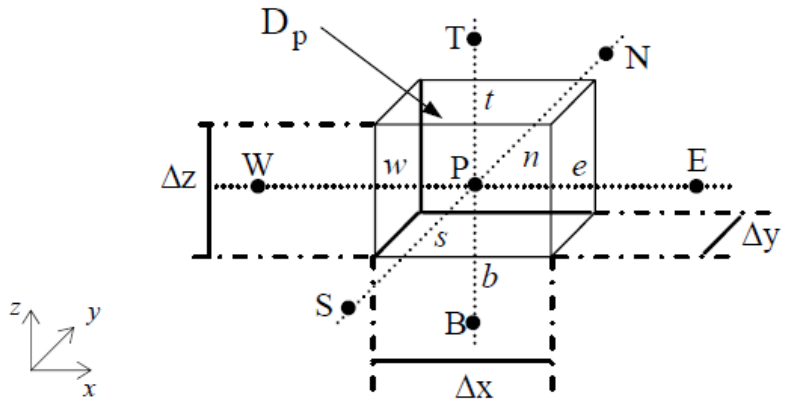

Fig II.3 Elementary volume Dp [CHE 07]

II.6 Principle of the finite volume method

The finite volume method is a powerful discretization method; it consists in using a simple approximation of the unknown to transform partial differential equations into an algebraic equation system. The resolution of equation (II.8) by the finite volume method consists first of all in subdividing the domain of study (Fig II.4), limited by the frontier Ω in elementary volumes of shape simple (rectangular two-dimensional). Each elementary volume is limited by four interfaces (e: Este, w: West, s: South, n: North) and surrounded by neighboring nodes (E 'East', W 'West', S 'South', N 'North') (Fig II.5). The second step consists of integrating equation (II.8) into the elementary volume that corresponds to the main node "P" [CHE 07].

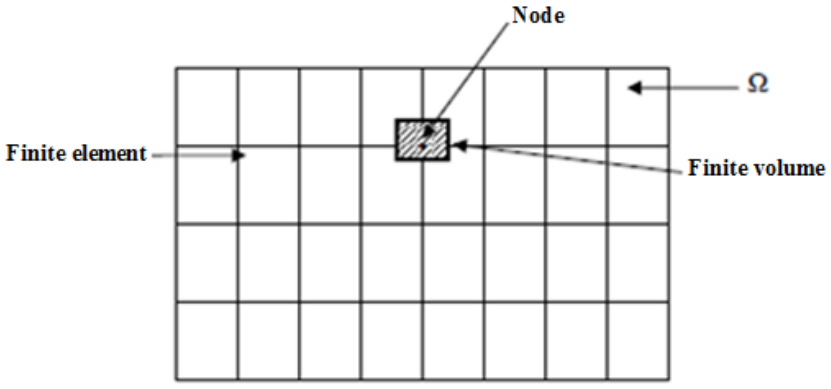

Fig.II.4 Mesh of the study domain

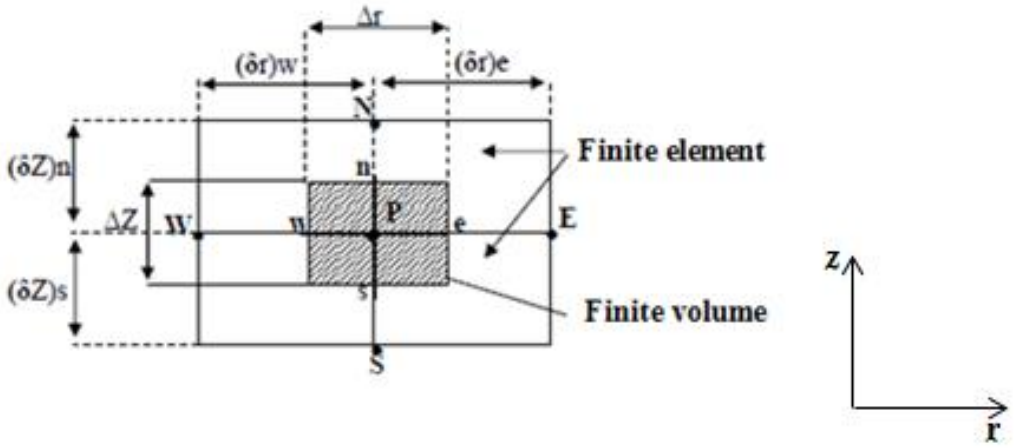

Fig.II.5 Description of a finite volume

Recall the magnetodynamic equation:

$$\frac{\partial}{\partial z}\left(\frac{1}{\mu r}\frac{\partial A^*}{\partial z}\right)+\frac{\partial}{\partial r}\left(\frac{1}{\mu r}\frac{\partial A^*}{\partial r}\right)-\frac{\sigma}{r}\frac{\partial A^*}{\partial t}=-J_s \tag{II.9}$$

By integrating the magnetodynamic equation on the finite volume corresponding to the node " P ", we obtain:

$$\int_r\int_z\left[\frac{\partial}{\partial z}\left(\frac{1}{\mu r}\frac{\partial A^*}{\partial z}\right)+\frac{\partial}{\partial r}\left(\frac{1}{\mu r}\frac{\partial A^*}{\partial r}\right)\right]drdz=\int_r\int_z\left[\frac{\sigma}{r}\frac{\partial A^*}{\partial t}-J_s\right]drdz \tag{II.10}$$

We pose:

- First term $$\int_r\int_z\left[\frac{\partial}{\partial r}\left(\frac{1}{\mu r}\frac{\partial A^*}{\partial r}\right)\right]drdz \tag{II.11}$$
- Second term $$\int_r\int_z\left[\frac{\partial}{\partial z}\left(\frac{1}{\mu r}\frac{\partial A^*}{\partial z}\right)\right]drdz \tag{II.12}$$
- Third term $$\int_r\int_z\left[\frac{\sigma}{r}\frac{\partial A^*}{\partial t}\right]drdz \tag{II.13}$$
- Source term $$-\int_r\int_z J_s drdz \tag{II.14}$$

The harmonic case the (II. 13) is becomes:

- Third term $$\int_r\int_z\left[\frac{\sigma}{r}(j\omega A^*)\right]drdz \tag{II.15}$$

II.6.1 Integration of the first term

The integral of the finite volume equation limited by the facets e, w, s and n is:

$$\int_w^e \int_s^n \frac{\partial}{\partial r}\left(\frac{1}{\mu r}\frac{\partial A^*}{\partial r}\right) dr dz = \int_s^n \frac{1}{\mu r}\frac{\partial A^*}{\partial r}\Bigg|_w^e dz \qquad \text{(II.16)}$$

It is assumed that the derivatives of the facet potential e and w are constant (II.16):

$$\int_s^n \frac{1}{\mu r}\frac{\partial A^*}{\partial r}\Bigg|_w^e dz = \left[\frac{1}{\mu r}\frac{\partial A^*}{\partial r}\Bigg|_e - \frac{1}{\mu r}\frac{\partial A^*}{\partial r}\Bigg|_w\right]\Delta z_p \qquad \text{(II.17)}$$

The basic idea of the FVM is to consider a linear variation of potential across facets e and w (Fig II.6), we can then write:

$$\left[\frac{1}{\mu r}\frac{\partial A^*}{\partial r}\Bigg|_e - \frac{1}{\mu r}\frac{\partial A^*}{\partial r}\Bigg|_w\right]\Delta z_p = \left[\frac{1}{\mu r_e}\left(\frac{(A^*)_E - (A^*)_p}{\Delta r_e}\right) - \frac{1}{\mu r_w}\left(\frac{(A^*)_p - (A^*)_W}{\Delta r_w}\right)\right]\Delta z_p \qquad \text{(II.18)}$$

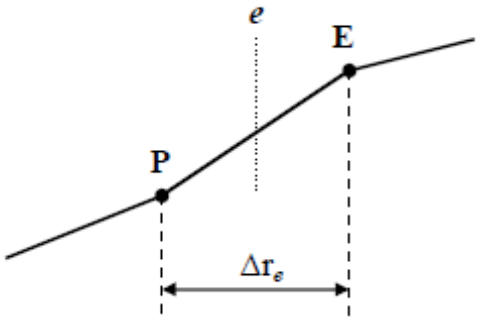

Fig II.6 Linear approximation of potential across the facet e

Replacing these derivatives in (II.17), we obtain the following linear combination:

$$a_e(\mathrm{A}^*)_E + a_w(\mathrm{A}^*)_W - (a_e + a_w)\mathrm{A}_p^* \qquad \text{(II.19)}$$

Where:

$$a_e = \frac{1}{\mu r_e}\frac{dz_p}{\Delta r_e} \qquad \text{(II.20)}$$

$$a_w = \frac{1}{\mu r_w}\frac{dz_p}{\Delta r_w} \qquad \text{(II. 21)}$$

$$\Delta r_e = \frac{\Delta r_E + \Delta r_P}{2} \tag{II.22}$$

$$\Delta r_w = \frac{\Delta r_w + \Delta r_P}{2} \tag{II.23}$$

For a regular mesh $(\Delta r_e = \Delta r_w = \Delta r_E = \Delta r_W = \Delta r_p = \Delta r)$, we obtain:

$$a_i = \frac{1}{\mu r_i}\frac{dz_p}{\Delta r_i} \text{ for } i = e, w \tag{II.24}$$

II.6.2 Integration of the second term

$$\int_w^e \int_s^n \frac{\partial}{\partial z}\left(\frac{1}{\mu r}\frac{\partial A^*}{\partial z}\right) dr dz = \int_w^e \frac{1}{\mu r}\frac{\partial A^*}{\partial z}\Big|_s^n dr = \left[\frac{1}{\mu r}\frac{\partial A^*}{\partial r}\Big|_n - \frac{1}{\mu r}\frac{\partial A^*}{\partial r}\Big|_s\right]\Delta r_p \tag{II.25}$$

In the same method we obtain the following linear combination:

$$a_n (A^*)_N + a_s (A^*)_S - (a_n + a_s) A_p^* \tag{II.26}$$

Where:

$$a_n = \frac{1}{\mu r_n}\frac{dz_p}{\Delta r_n} \tag{II.27}$$

$$a_s = \frac{1}{\mu r_s}\frac{dz_p}{\Delta r_s} \tag{II.28}$$

$$\Delta r_n = \frac{\Delta r_N + \Delta r_P}{2} \tag{II.29}$$

$$\Delta r_s = \frac{\Delta r_S + \Delta r_P}{2} \tag{II.30}$$

For a regular mesh:

$$a_i = \frac{1}{\mu r_i}\frac{dz_p}{\Delta r_i} \text{ for } i = n, s \tag{II.31}$$

II.6.3 Integration of the third term

$$\int_w^e \int_s^n \frac{\sigma}{r}\left(j\omega A^*\right) dr dz = \frac{j\omega\sigma_p}{r} A^* \Delta r_p \Delta z_p \tag{II.32}$$

In the same method we obtain the following linear combination:

$$a_m A_p^* \tag{II.33}$$

Where:

$$a_m = \frac{j\omega\sigma_p}{r}\Delta r_p \Delta z_p \tag{II.34}$$

II.6.4 Integration of the source term

$$\int_w^e \int_s^n J_s dr dz = J_s \Delta r_p \Delta z_p \tag{II.35}$$

After calculating the set of terms from equation (II. 10), we obtain the algebraic equation given by (II.36). This expression gives the magnetic vector potential at node P as a function of potentials at neighboring nodes.

$$A_P^* = (\frac{1}{a_P})(a_e A_E^* + a_w A_W^* + a_s A_S^* + a_n A_N^* + C_s) \tag{II.36}$$

Where:

$$a_P = a_e + a_w + a_n + a_s + j\omega\frac{\sigma_P}{r_P} \tag{II.37}$$

$$C_s = J_s \Delta r_p \Delta z_p \tag{II.38}$$

II.7 Boundary conditions

For the resolution of electromagnetic partial differential equations, we must to associate the boundary conditions with these equations.

In electromagnetism we take two conditions types:

II.7.1 Dirichlet boundary condition

It imposes the values of the magnetic vector potential $\vec{A}$ at the edges of study domain; these values are taken zero ($\vec{A} = \vec{0}$) by the consideration of the infinite.

II.7.2 Neumann boundary condition

It is used in the case where the system to be studied presents symmetry planes. The problem imposes the values of $\vec{A}$ at the edges of the domain and that of $\frac{\partial \vec{A}}{\partial \vec{n}}$ at the levels of the planes of symmetry ($\vec{n}$ represents the normal with the plane of section).

II.8 Numerical methods for solving systems of linear algebraic equations

For solving systems of algebraic equations, there are two main families of methods:

- Direct methods
- Iterative methods.

Direct methods are applicable for linear systems where the number of elements is reduced. They are precise is exact but require a lot of memory space and computing time, among the direct methods we mention the Cramer method, Gauss method and Jordon method. In practice, the iterative methods that are used the most and especially for algebraic systems. The principle of iterative methods consists in passing from an estimate $X^{(k)}$ of the solution to another estimate $X^{(k+1)}$ of this solution. If convergence occurs, the solution can be only reached after a number of iterations. Among these methods, we cite: Jacobi method, Gauss-Seidel method and the relaxation method.

II.8.1 Jacobi method

It based on the system transformation: A. X= [B] into:

$$X_i^{(k+1)} = \left[b_i - \sum a_{ij} X_j^k \right] \Big/ a_{ij} \ ; (\mathrm{i} \neq \mathrm{j}),\ i = 1,.....n \qquad \text{(II. 39)}$$

An initial arbitrary value X_i^0 is estimated for (k = 0)

The calculation will be stopped if:

$$\left| X_i^{(k+1)} - X_i^k \right| < \varepsilon \ \text{ Where } \frac{\left| X_i^{(k+1)} - X_i^k \right|}{X_i^k} < \varepsilon \qquad \text{(II. 40)}$$

ε : User-imposed precision.

II.8.2 Gauss-Seidel method

This method consists of transforming the system A. X = B into:

$$X_i^{(k+1)} = \left[b_i - \sum_{j=1}^{(i-1)} a_{ij} X_j^{(k+1)} - \sum_{j=(i+1)}^{n} a_{ij} X_j^{k} \right] \Big/ aij \,, i = 1, \ldots\ldots\ldots n \qquad \text{(II.41)}$$

By giving the unknowns X_i^k initial arbitrary values X_i^0 for (k = 0)

The calculation will be stopped if:

$$\left| X_i^{(k+1)} - X_i^k \right| < \varepsilon \text{ Where } \frac{\left| X_i^{(k+1)} - X_i^k \right|}{X_i^k} < \varepsilon \qquad \text{(II.42)}$$

ε : User-imposed precision.

II.8.3 Relaxation method

To improve the convergence speed in the iterative methods, a relaxation factor λ is used.

$$X_i^{(k+1)} = X_i^k + \lambda (X_i^{(k+1)} - X_i^k) \qquad \text{(II.43)}$$

II.9 Impedance calculation of an eddy current sensor

The study of approaches to calculation of sensor impedance is very important. An eddy current sensor utilizes the variation of sensor impedance to perform the measurement of physical parameters, and the sensor impedance is an important parameter for investigating the properties of an eddy current sensor. The knowledge of analytical expressions for the electromagnetic (EM) fields produced by the sensors used in eddy current testing is an important point in the development and application of these devices. The vector potential formulation is used for the calculation of the fields.

The impedance of the sensor can be calculated by the Faraday law and the Stokes theorem [STA 92, WIL 00]

$$Z = \frac{V}{I} = \frac{E_{fem}}{I} \qquad \text{(II.44)}$$

E_{fem} : Electromotive force.

I: Supply current.

$$Z = \frac{\oint \mathrm{E}\ \mathrm{dl}}{\int_S \mathrm{J}\ \mathrm{dS}} = \frac{-\partial_t \iint \mathrm{B}\ \mathrm{ds}}{\int_S \mathrm{J}\ \mathrm{dS}} = \frac{-\partial_t \iint (\ \mathrm{rot}\ \mathrm{A}\ ) \mathrm{ds}}{\int_S \mathrm{J}\ \mathrm{dS}} = \frac{-\partial_t \oint \mathrm{A}\ \mathrm{dl}}{\int_S \mathrm{J}\ \mathrm{dS}} \quad \text{(II.45)}$$

A: Magnetic vector potential.

If the magnetic induction is sinusoidal function, then:

$$Z = \frac{-j\ \omega \oint \mathrm{A}\ \mathrm{dl}}{\int_S \mathrm{J}\ \mathrm{dS}} \quad \text{(II.46)}$$

For determine the imaginary and actual parts of the impedance Z of the sensor we must calculating the energy stored throughout the space and Joule losses in the conductive plate

✓ Determination of the reactance X (imaginary part):

$$E_{em} = \frac{1}{2} \int_\Omega B\ H\ d\ \Omega \quad \text{(II.47)}$$

$$E_{em} = \frac{1}{2} L\ I^2 \quad \text{(II.48)}$$

$$X = L\omega \quad \text{(II.49)}$$

Where:

Ω : Domain of study.

E_{em} : stored magnetic energy.

L : Inductance of the sensor.

We combine the equations (II.47), (II.48), (II.49) and (II.5), obtain:

$$X = \frac{1}{I^2}\ \omega \int_\Omega \frac{1}{\mu}\ (B)^2\ d\Omega \quad \text{(II.50)}$$

✓ Determination of the resistance R (real part):

$$E_{Joule/\,plate} = R_{plate} I_{ind}^2 \quad \text{(II.51)}$$

$$E_{Joule/sensor} = R_{sensor} I_{ind} \quad \text{(II.52)}$$

$$R_{plate} = \frac{1}{\sigma}\ \frac{l}{S} \tag{II.53}$$

$$I_{ind} = J_{ind}\ S \tag{II.54}$$

I_{ind}, J_{ind} are the currents and the density of the eddy currents.

We combine the equations (II. 51), (II. 52), (II. 53) and (II. 54), obtain:

$$R = \frac{1}{I^2}\ \int_{\Omega}\frac{1}{\sigma}\ J_{ind}^2\ d\Omega \tag{II.55}$$

II.10 Modeling the problem

The corresponding problem is illustrated in (Fig II.7), it is of axisymmetric type consisting of a plate placed between two eddy current sensors; the sensor 1 has 800 turns and the sensor 2 has 120 turns. The chosen thickness of the plate for such modeling is e = 10.2mm. The dimensions of the different elements constituting this problem are shown in Table II.1.

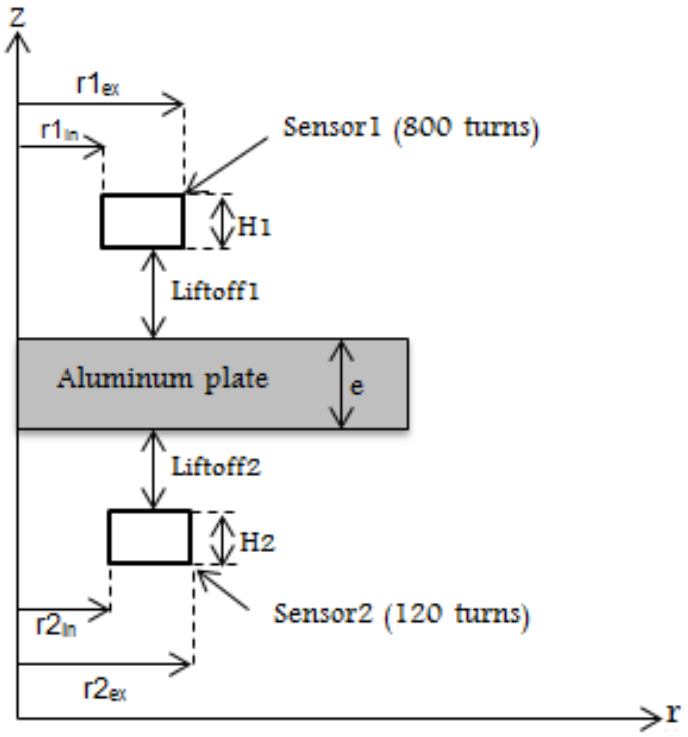

Fig II.7 Axisymmetric geometric model of the problem

Table II.1 Dimensions of the problem, in mm

Sensor 1 (800 turns)	Exterior diameter	09
	Interior diameter	02
	Height	01.5
	Thickness of a layer	0.07
Sensor 2 (120 turns)	Exterior diameter	10
	Interior diameter	02
	Height	01.5
	Thickness of a layer	00.2

Fig II.8 and Fig II.9 show respectively the reactance variation and the resistance variation for different Liftoff and for frequencies from 10 KHz to 500 KHz. These variations are relative to the sensor 1, of 800 turns.

Also for the sensor 2 of 120 turns, Fig II.10 and Fig II.11 show respectively the reactance variation and the resistance variation for different Liftoff and for frequencies from 10 KHz to 500 KHz.

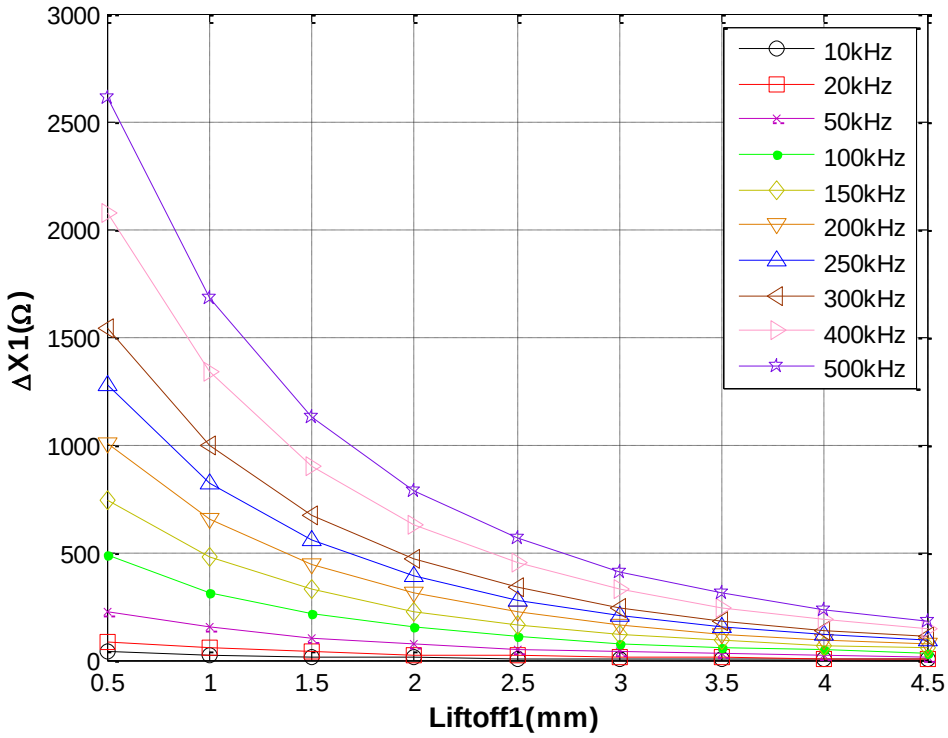

Fig II.8 Reactance variation for different frequencies (Sensor 1)

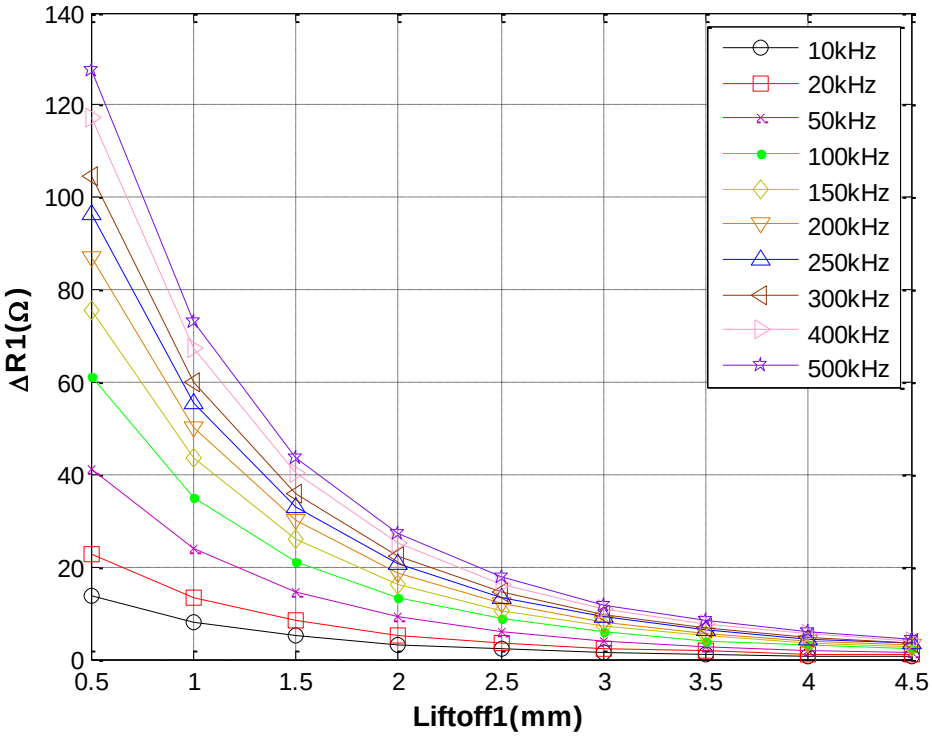

Fig II.9 Resistance variation for different frequencies (Sensor 1)

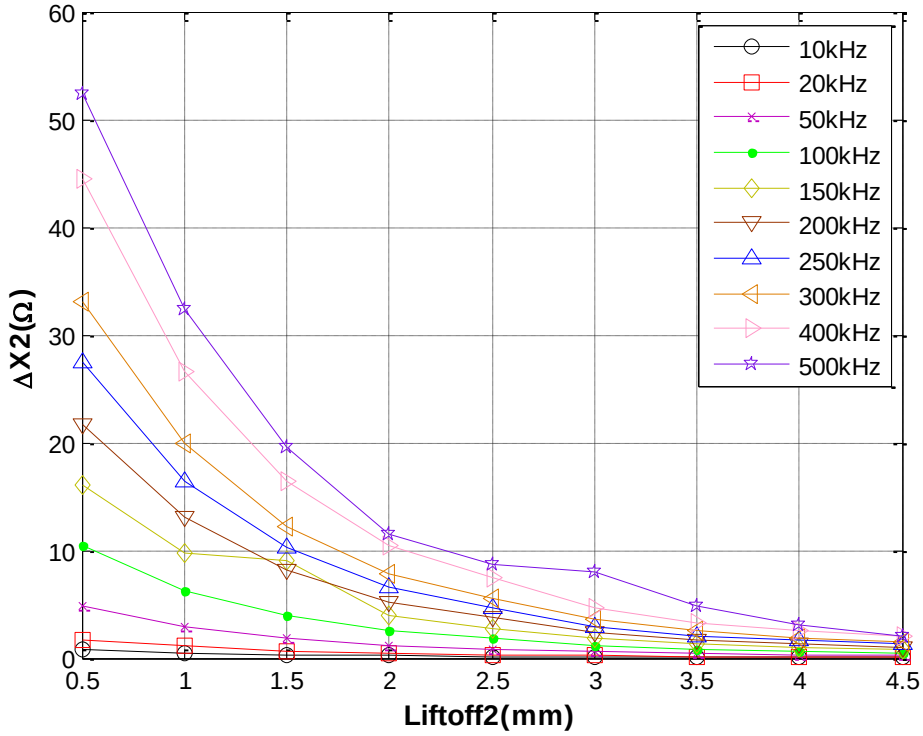

Fig II.10 Reactance variation for different frequencies (Sensor 2)

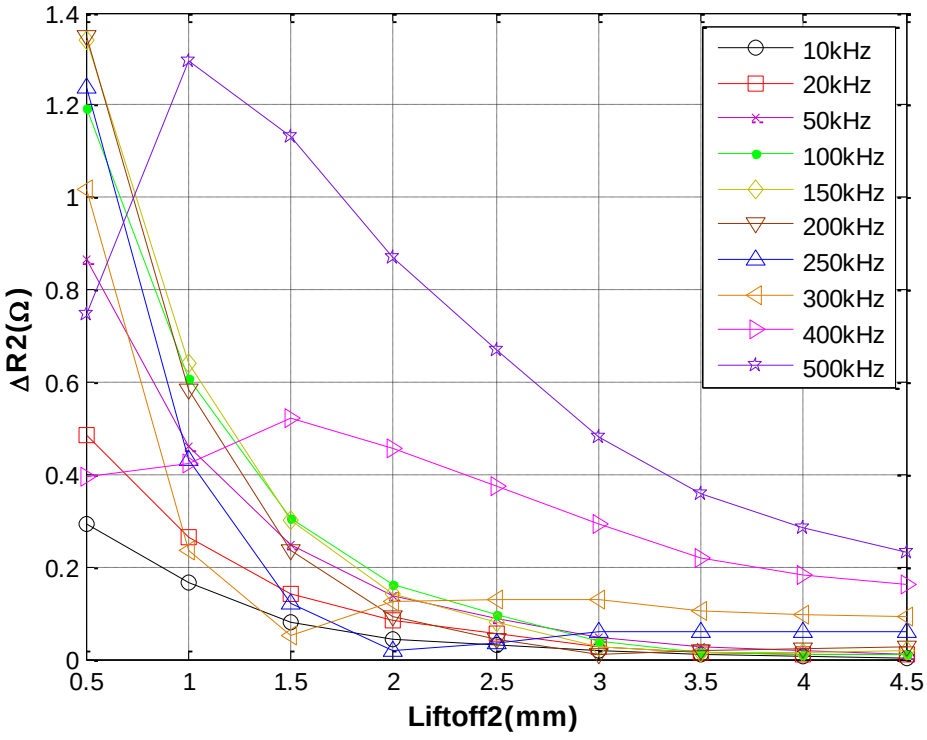

Fig II.11 Resistance variation for different frequencies (Sensor 2)

The results of this modeling (the reactance variation and the resistance variation for different Liftoff and for different frequencies), gave us an overall idea about the sensors sensitivities. These variations are to be validated experimentally in the next chapter, and followed by experimental analysis of sensors sensitivities 1 and 2.

II.11 Conclusion

In this chapter we presented the formulations as well as the magnetodynamic model. In consideration of the type of application to be treated, the cylindrical axisymmetric case has been detailed; As well as the presentation of different techniques resolution of partial differential equations (PDE). Here, the finite volume method (FVM) was chosen for the transformation of PDE into algebraic equations. The resolution method adopted from the algebraic system resulting from the discretization of the magnetic potential formulation by FVM is the Gauss-Seidel method. Second part of this chapter, we treat the modeling in the case 2D axisymmetric by the finite volume method FVM.

Chapter III
Application: Thickness evaluation of thick aluminum plates

III.1 Introduction

In the previous chapter, we presented to a field calculation by the finite volume method FVM to calculate the impedance variations of two eddy current sensors as a function of the desired thickness of the plate and that by exploiting the variations of the two Liftoff on both sides of the plate. The objective of this work is to propose an alternative method for thickness measurement of thick metallic plates based on bi-eddy current sensor. In this chapter, we will realize the test bench for the thickness measurement of thick metallic plates, the measurement system is mainly composed of two eddy current sensors, an impedance analyzer LCR-meter and a personal computer equipped with the Labview software.

III.2 Measurement procedure

As schematized in (Fig III.1), the measurement system is mainly composed of two eddy current sensors, an impedance analyzer LCR-meter and a personnel computer equipped with the Labview software. The thick metallic plate we want to measure its thickness ‘e’ is placed between the two sensors. Note that both eddy current sensors are fixed with a distance ‘L’ between them. The measurement instrument LCR-meter ensures the connection between both sensors and the personnel computer. The measured impedances of the two sensors are translated from the LCR-meter to the developed Labview application.

The measurement procedure can be summarized as following. Firstly the calibration step, so the reactances of both sensors are measured without the metallic plate; these reactances are saved and symbolized by X1_0 and X2_0 in the Labview application. Once the metallic plate is placed between the sensors, a change in both reactances will be noted; these new reactances are saved and symbolized by X1 and X2. We define by ΔX1 the reactance variation of sensor 1, and by ΔX2 the reactance variation of sensor 2. These reactance variations are calculated as the difference between the two cases with and without plate. On the basis of the following relationship, one can calculate the plate thickness ‘e’ as:

$$e = L - \left[\widetilde{Liftoff1} + \widetilde{Liftoff2}\right] \quad \text{(III.1)}$$

$\widetilde{Liftoff1}$ and $\widetilde{Liftoff2}$ are the transfer functions relating to the sensors 1 and 2, ‘Two functions which returns the value of the Liftoff according to the reactance variation or the resistance variation.

Both transfer functions $\widetilde{Liftoff1}$ and $\widetilde{Liftoff2}$ has to be determined experimentally in the next section.

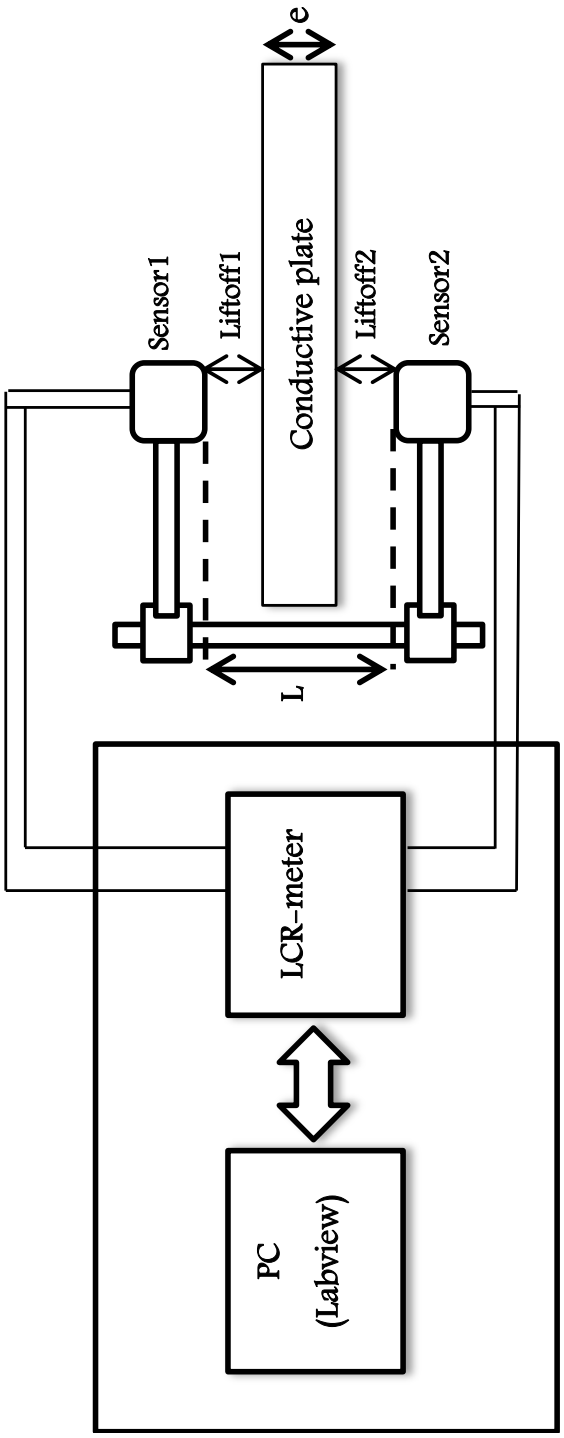

Fig III.1 Schematization of the measurement system

III.3 Experimental part

III.3.1 Measurement of the impedance variation of the sensors

As indicated, two eddy current sensors were used to measure the thickness of the plate. However, several plastic shims of thickness 0.23mm are used as variable Liftoff; these shims are inserted between the sensor and the plate for both sides of the plate (Fig III.2), the reactance and the resistance of the two sensors are measured by LCR-meter (Fig III.3) for different frequencies ranging from 10 kHz to 500 kHz. (Fig III.4) and (Fig III.5) show respectively the reactance variation (ΔX1) and the resistance variation (ΔR1) of sensor 1 for different values of Liftoff1 ranging from 0.23mm to 20×0.23mm. (Fig III.6) and (Fig III.7) respectively show the reactance variation (ΔX2) and the resistance variation (ΔR2) of sensor 2 for different values of Liftoff2.

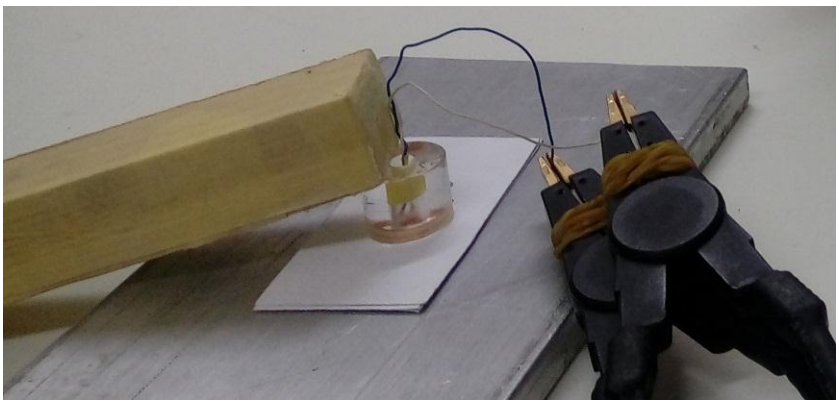

Fig III.2 Insertion of shims to vary the Liftoff

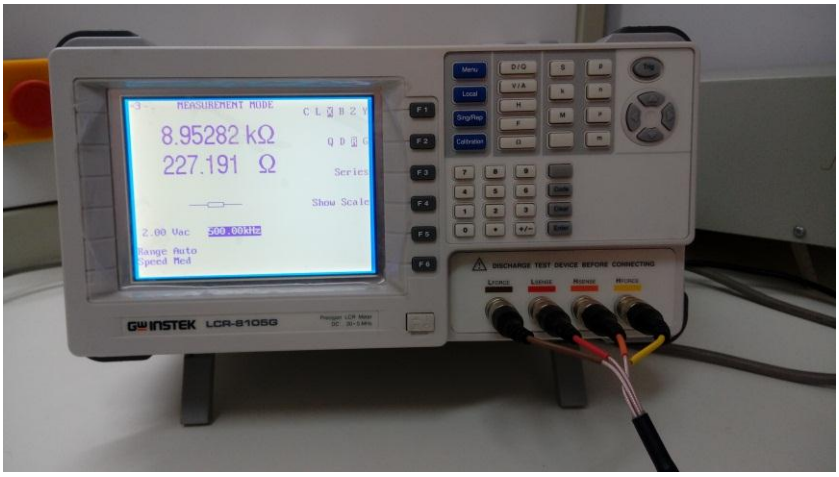

Fig III.3 LCR-meter used for measuring impedances

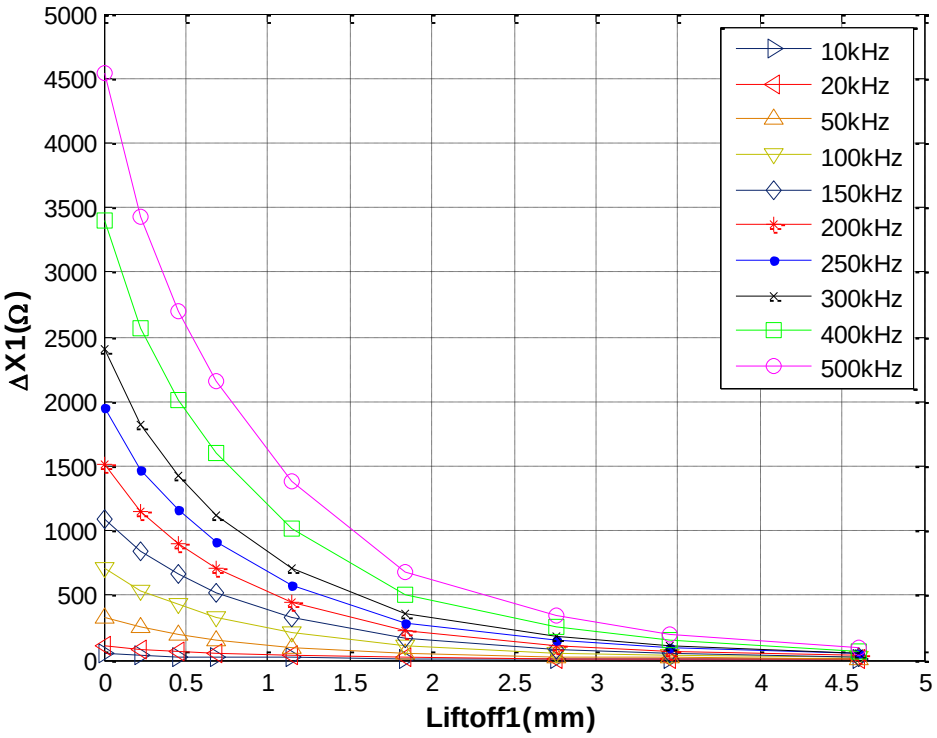

Fig III.4 Measurement of the reactance variation for different frequencies (Sensor1)

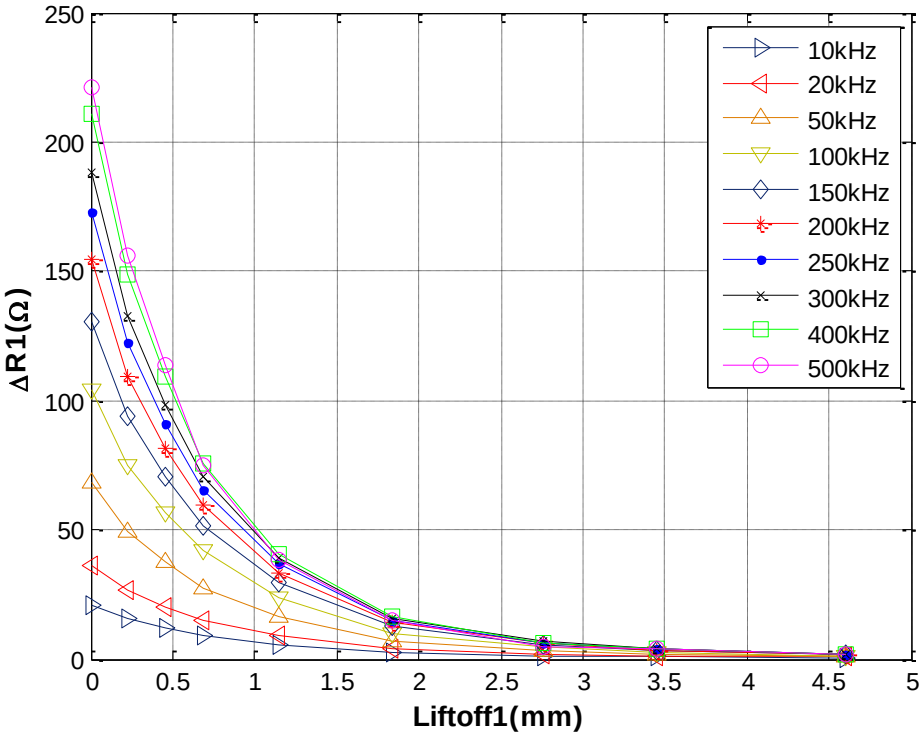

Fig III.5 Measurement of the resistance variation for different frequencies (Sensor1)

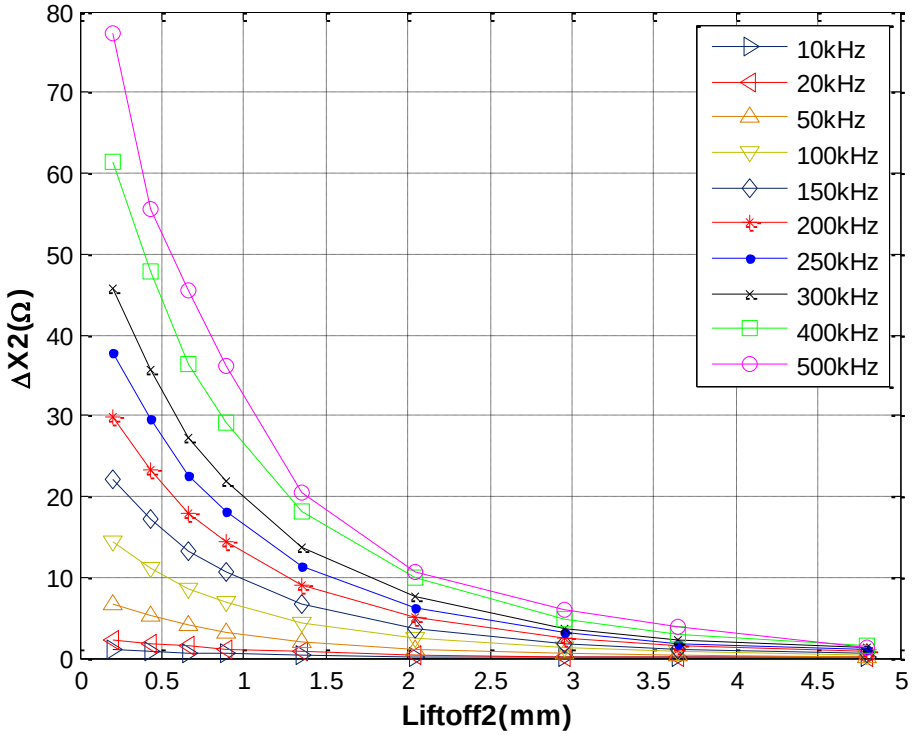

Fig III.6 Measurement of the reactance variation for different frequencies (Sensor2)

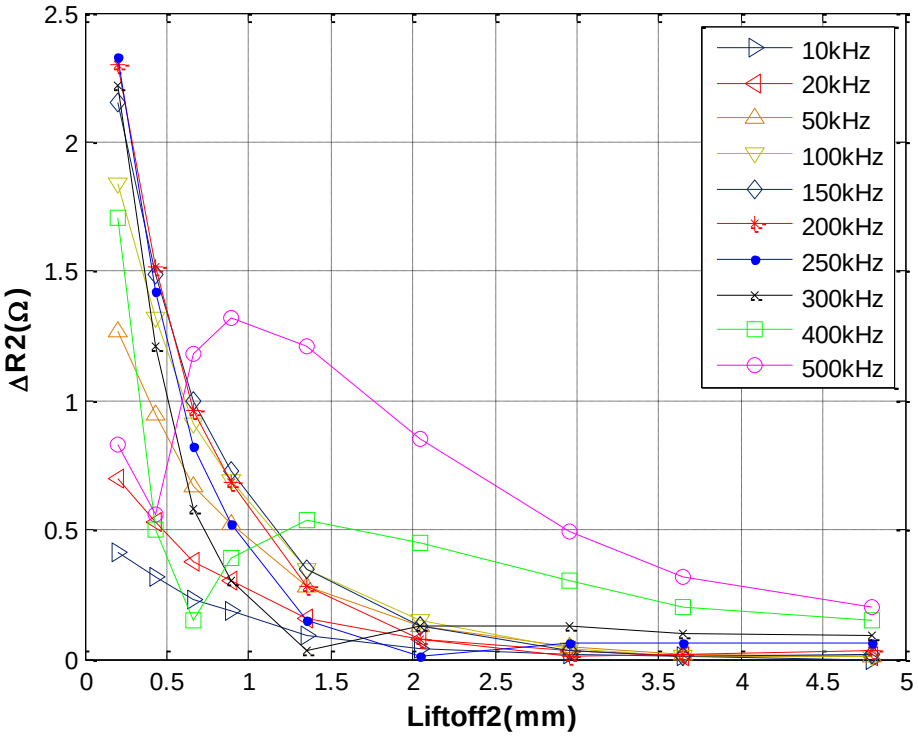

Fig III.7 Measurement of the resistance variation for different frequencies (Sensor2)

Actually, the evaluation of the four preceding variations (Fig III.4, Fig III.5, Fig III.6 and Fig III.7) aims to determine the previously announced transfer functions. To reach this objective, it is very convenient to carry out a sensitivity analysis of the sensors.

III.3.2 Sensitivity analysis of the sensors

We are interested here in calculating the sensitivity of the two sensors vis-à-vis the reactance and resistance variations. In general, the sensitivity (S) is defined by 'the ratio between two successive measurements of the reactance (or resistance)' and 'the difference between the two corresponding Liftoff':

$$S = \frac{\Delta F}{\Delta(\text{Liftoff})} \tag{III.2}$$

F is either the reactance variations (ΔX) or the resistance variations (ΔR). For example the sensitivity of sensor 1 with respect to ΔX, equation (III. 2) is rewritten as follows:

$$S_{\Delta X}^{1} = \frac{\Delta(\Delta X1)}{\Delta(\text{Liftoff } 1)} \tag{III.3}$$

So, by using the experimental results previously given by (Fig III.4, Fig III.5, Fig III.6 and Fig III.7), one can easily compute both sensors sensitivities by means of the general equation (III. 2). (Fig III.8, Fig III.9, Fig III.10 and Fig III.11) show respectively, the sensitivities of sensor 1 and sensor 2.

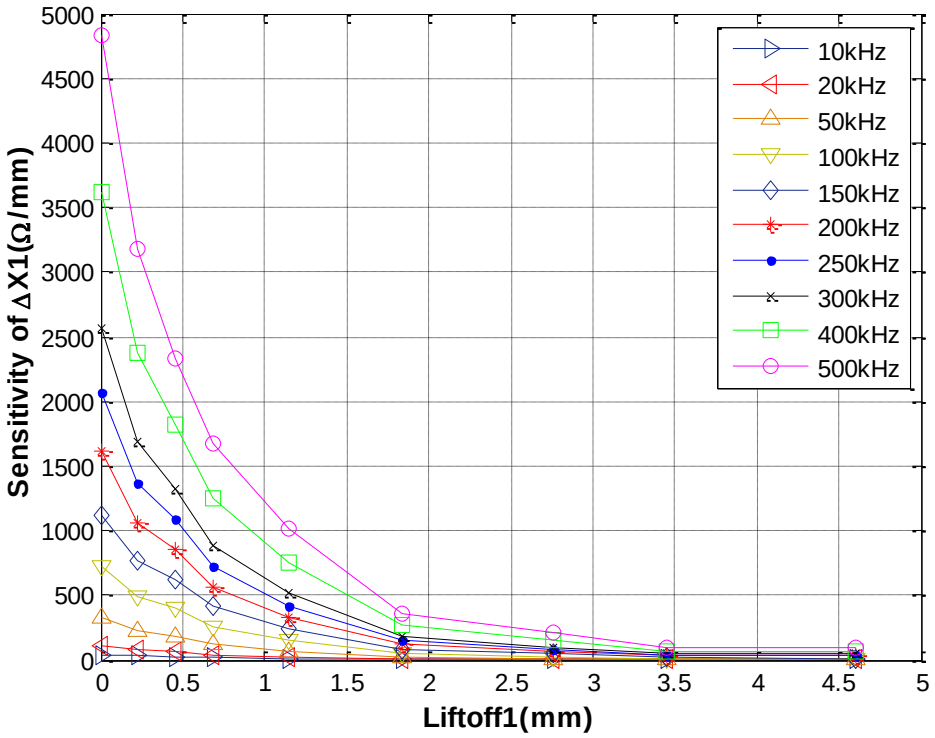

Fig III.8 Sensitivity of the sensor 1 vis-à-vis the reactance variation

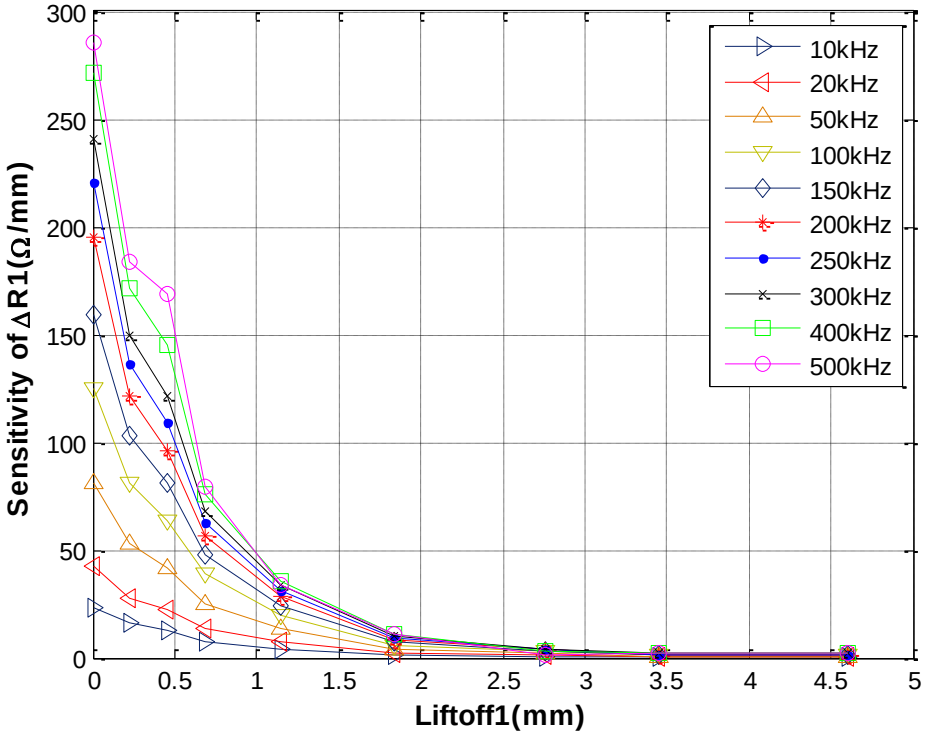

Fig III.9 Sensitivity of the sensor 1 vis-à-vis the resistance variation

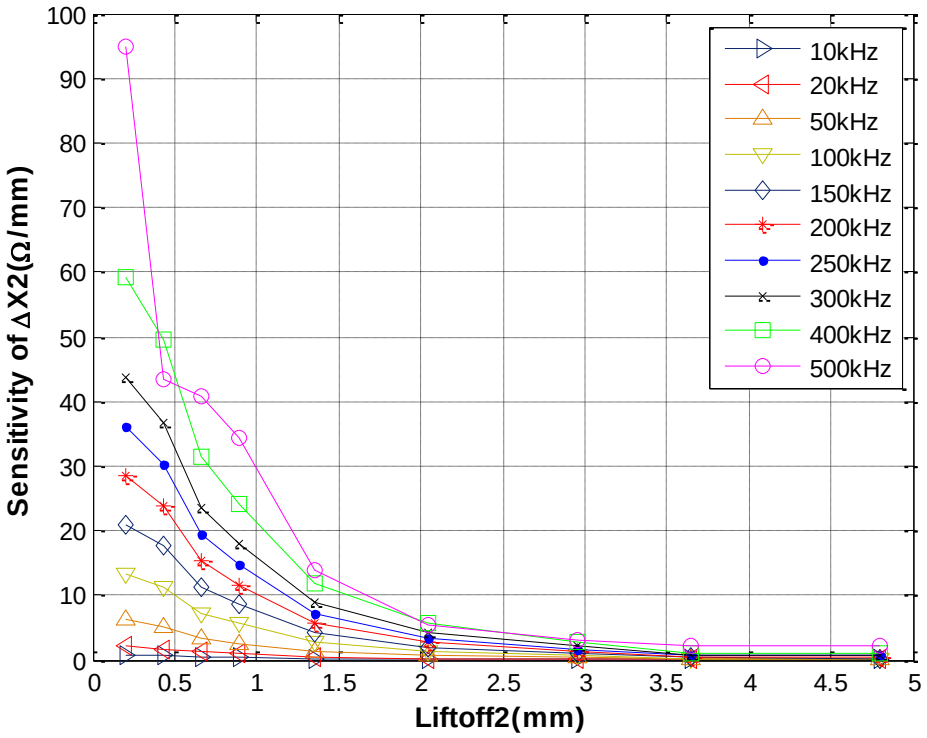

Fig III.10 Sensitivity of the sensor 2 vis-à-vis the reactance variation

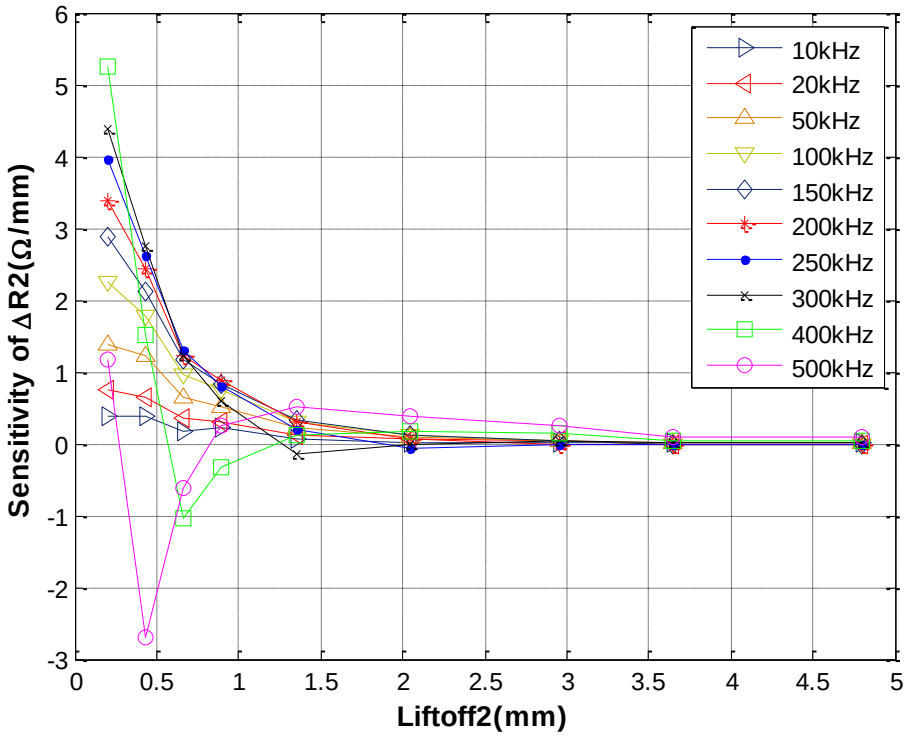

Fig III.11 Sensitivity of the sensor 2 vis-à-vis the resistance variation

From these sensitivity characteristics (Fig III.8, Fig III.9, Fig III.10 and Fig III.11), we can see that:

- ✓ The 500 kHz frequency has better sensitivity in all cases.
- ✓ A low sensitivity of both sensors with respect to the resistance variations ΔR.
- ✓ A high sensitivity of both sensors is observed with respect to the reactance variations ΔX.

As a result, thereafter only the reactance variation of which has a better sensitivity is taken into account. Also, this sensitivity analysis allowed us to choose the working frequency which is 500 kHz; a reasonable frequency respecting the electrical characteristics of the sensors.

III.3.3 Transfer functions determination

Consider only the reactance variation ΔX; the previous experimental measurements are reproduced as shown in (Fig III.12 and Fig III.13) by using a polynomial interpolation of degree three, which appears sufficient, these two last figures can be approximated by the following two equations:

$$\widetilde{\text{Liftoff1}} = a1(\Delta X1)^3 + b1(\Delta X1)^2 + c1(\Delta X1) + d1 \quad \text{(III.4)}$$

$$\widetilde{\text{Liftoff2}} = a2(\Delta X2)^3 + b2(\Delta X2)^2 + c2(\Delta X2) + d2 \quad \text{(III.5)}$$

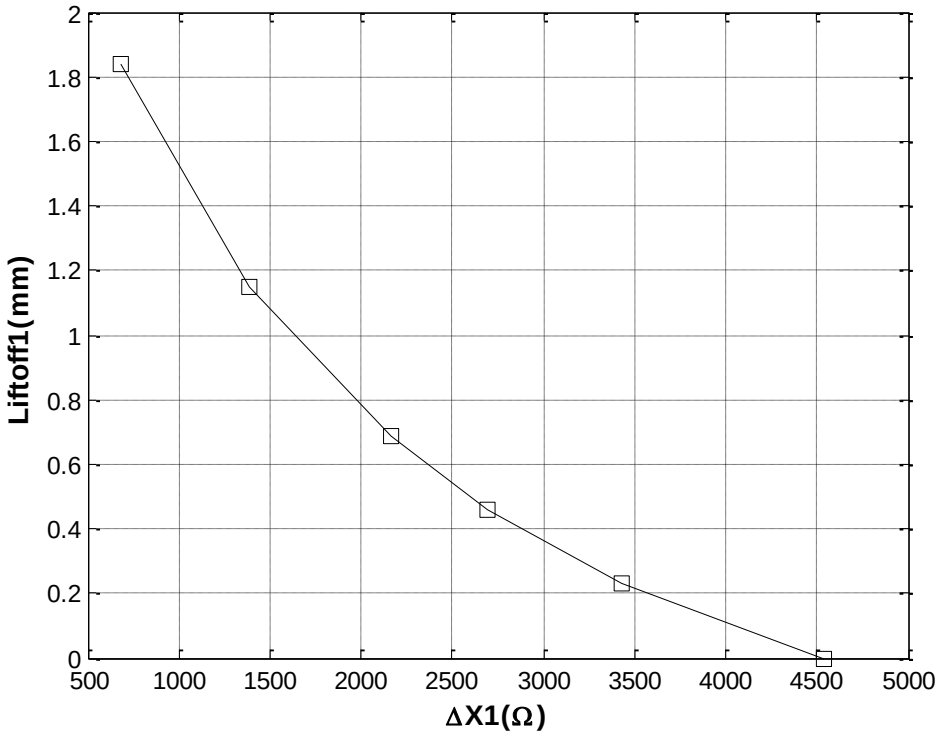

Fig III.12 Liftoff as function of ΔX for sensor 1

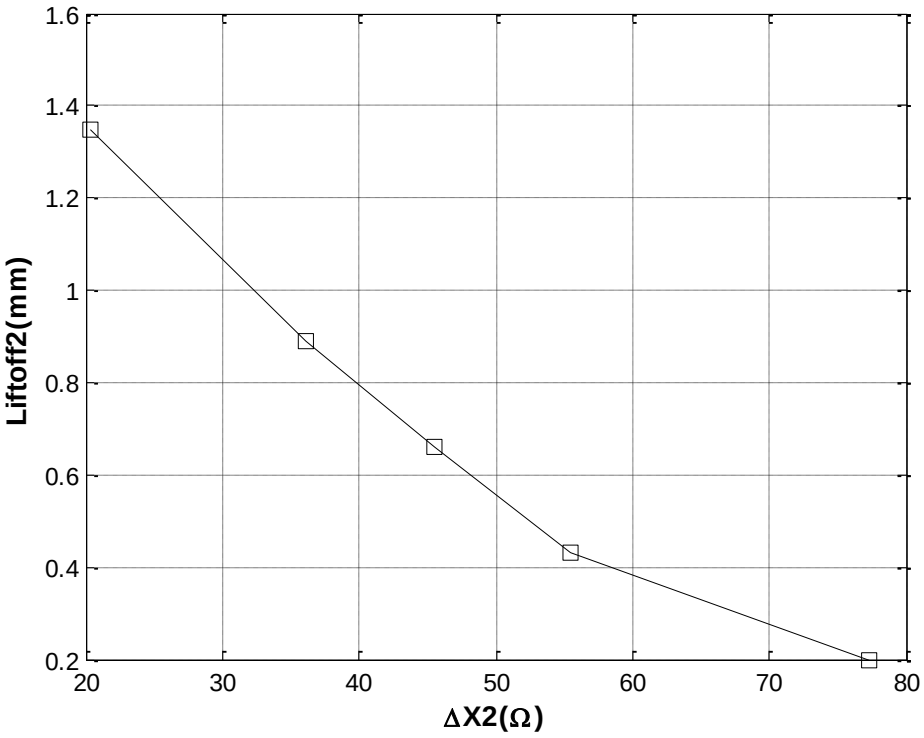

Fig III.13 Liftoff as function of ΔX for sensor 2

The eight coefficients a1, b1, c1, d1, a2, b2, c2 and d2 in these polynomial equations are given by using the experimental data of (Fig III.12 and Fig III.13) by the function Matlab 'polyfit'. Indeed, equations (III.4) and (III.5) are the so-called looking for transfer functions which represent the main components of this proposal; using the points illustrated in Tables III.1 and III.2. These coefficients are shown in Table III.3.

Table III.1 Points used to determine sensor 1 transfer function

Liftoff1(mm)	0	0.23	0.46	0.69	1.15	1.84
ΔX1(Ω)	4543	3430	2698	2161	1384	683

Table III.2 Points used to determine sensor 2 transfer function

Liftoff2(mm)	0	0.43	0.66	0.89	1.35	2.04
ΔX2(Ω)	77.35	55.50	45.54	36.17	20.37	10.76

Table III.3 The calculated values of the different coefficients

a1	b1	c1	d1
$-3.1271.10^{-11}$	$3.6638.10^{-7}$	-0.0024	4.0994
a2	b2	c2	d2
$-9.6017.10^{-6}$	0.0019	-0.1274	3.7273

III.3.4 Test bench and measurement protocol

Fig III.14 represents the test bench realized at the laboratory LGEB of Biskra, its constitutive elements are:

- Two eddy current sensors of 800turns and 120turns.
- Impedance Analyzer, it is LCR-meter of type GWInstek8105G.
- Pc equipped with Labview software.
- Measuring plate, Aluminum.

The two eddy current sensors are fixed on a millimetric graduated support, with a distance 'L' between them. The measurement instrument LCR-meter ensures the connection between both sensors and the personnel computer.

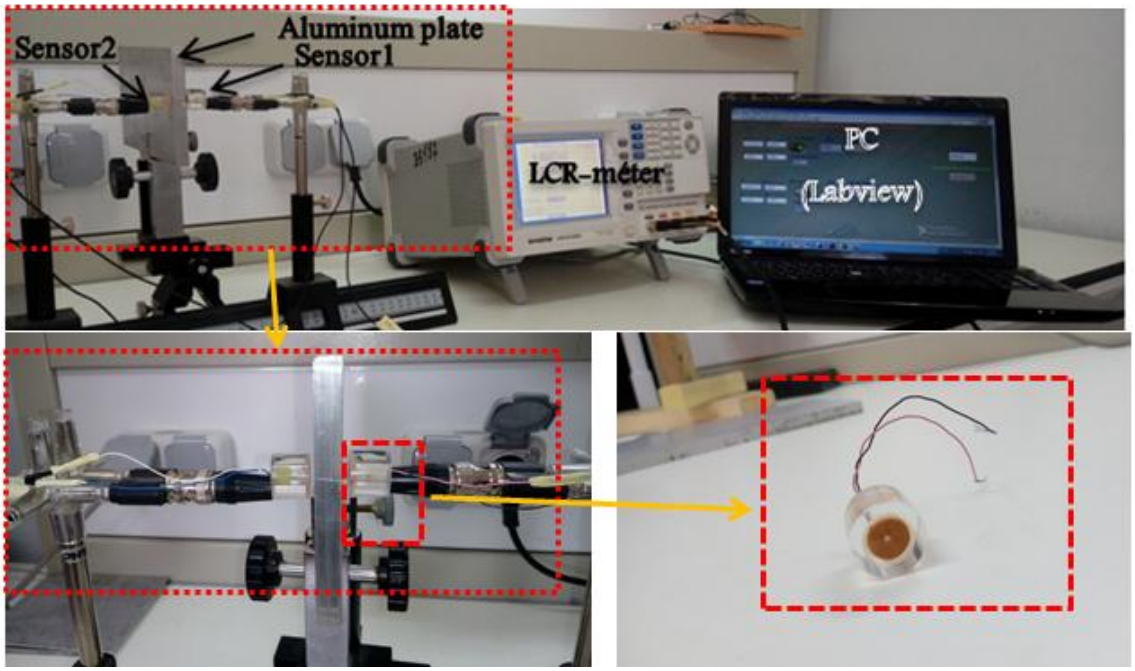

Fig III.14 Test bench at LGEB laboratory in Biskra

(Fig III.15) shows the front-panel of the developed Labview application and as illustration (Fig III.16) shows the Labview block diagram of equation (III.4); and in (Fig III.17) which represents the Labview block diagram of equation (III.1).

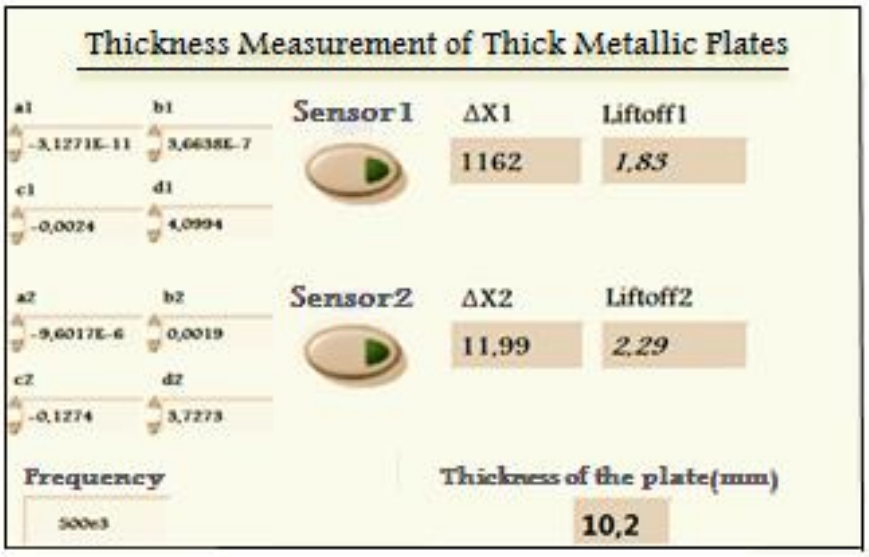

Fig III.15 Front-panel of the developed Labview application

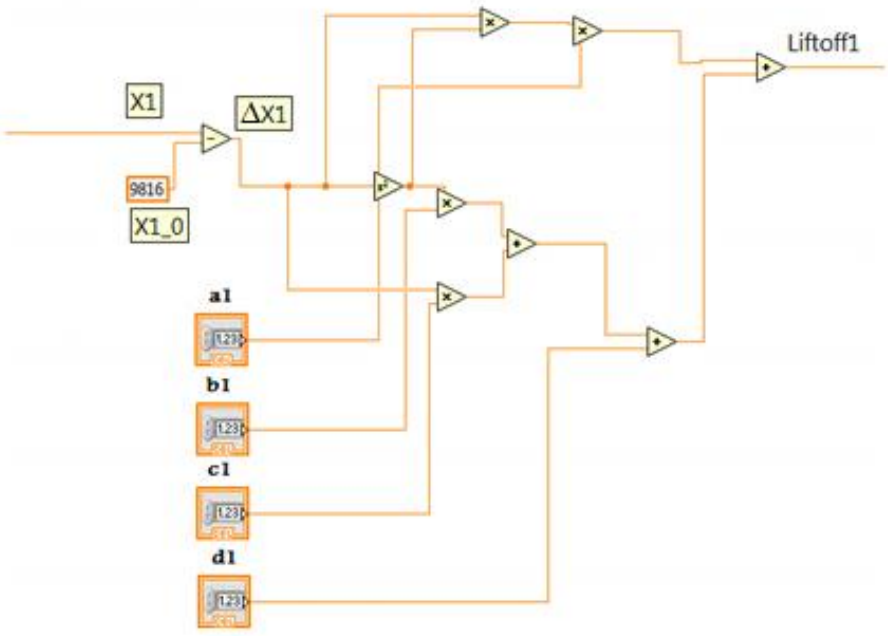

Fig III.16 Labview block diagram of equation (III. 4)

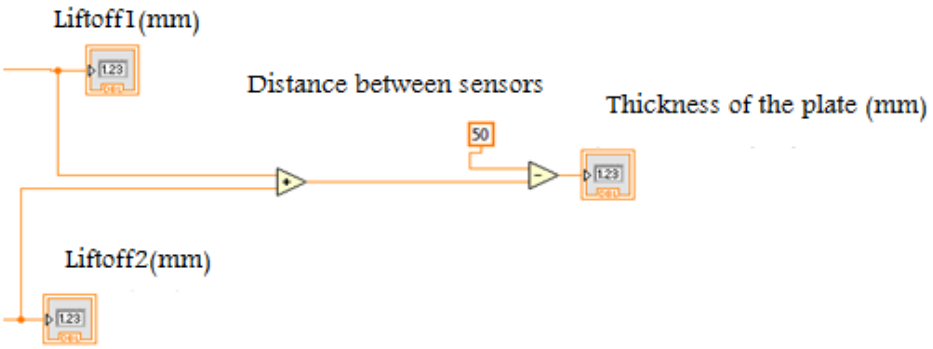

Fig III.17 Labview block diagram of equation (III.1)

In order to carry out the measurement, one can place the aluminum plate between the two sensors; knowing that it is not necessary to place it in the middle between the sensors i.e. Liftoff1 and Liftoff2 can be unequal. For a given plate, note that the value Liftoff1 + Liftoff2 do not change even when the plate moves between the sensors, thus the movement of the plate is canceled. Thickness computation is performed automatically, and the thickness value ‘e’ is displayed on the front-panel of the Labview application. The measurement can be carried out in real time, by replacing the actual plate by another; we obtain the new corresponding thickness displayed on the screen.

To start a measurement, simply:

- Run the Labview application,
- Display the front -panel of the Labview application (interface),
- On this same interface, set the frequency to 500kHz and enter the 8 coefficients of the transfer functions,
- Click on the control button 'Sensor1', then 'Sensor2' to record the reactance values of the two sensors, without the presence of the plate to be measured (empty measurement),
- Place the plate between the two sensors, and click on the control buttons again. Both Liftoff (Liftoff1 and Liftoff2) and the plate thickness 'e' are immediately displayed on the interface.

III.3.5 Experimental results

Three thick aluminum plates with different thicknesses of 2.2mm, 5.1mm and 10.2mm are prepared and measured (Table III.4). From the results, one can observe a small measurement error validating our proposition.

Table III.4 Summary of the thickness measurement

Measured thickness (mm)	Exact thickness (mm)	Relative error (%)
10.25	10.20	00.50
05.09	05.10	00.20
02.18	02.20	01.00

III.4.Conclusion

This chapter deals with a bi-eddy current sensor based scanning system for thickness evaluation of thick metallic plates. The realized system takes place when continuous and real time monitoring of thickness measurement is required. The procedure was experimentally validated using a set of thick plates made of aluminum, and a good accuracy has been obtained.

GENERAL CONCLUSION

General Conclusion

This work presented is part of the practical realization of an experimental test bench for thicknesses of thick metallic plates. Actually, this work proposes an alternative method for thickness evaluation of thick metallic plates using eddy currents. The proposed method involves Liftoff measurement of a bi-eddy current sensor. The main components of the system proposed and realized are two eddy current sensors, an aluminum plate, LCR-meter and a PC equipped with Labview software. An experimental test bench was carried out at LGEB laboratory in Biskra. The realized system takes place when continuous and real time monitoring of thickness measurement is required. The procedure was experimentally validated using a set of thick plates made of aluminum, and a good accuracy has been obtained.

This work also the subject of a field calculation by the finite volume method FVM as well as the evaluation of the impedance variation of the two sensors as a function of the plate thickness is placed between them. For this, an axisymmetric magnetodynamic model of the corresponding problem has been developed.

For test the proposed measurement system, several aluminum plates with different thicknesses in the range of 2mm to 10mm are prepared and measured. The measured thicknesses compared to the exact thicknesses, show a good accuracy of the experimental bench whose maximum relative error does not exceed 1%. The methodology proposed in this work can be applied for different inductive sensors and for other types of materials. As a perspective, we are going to extend this technique for rapid and accurate measurement of thick metallic tubes.

BIBLIOGRAPHICAL REFERENCES

Bibliographical references

[ABD 98] **R. Abdessemed, M.S. Aggoune, F.Z. Kadid**, "Magnétisme", Physique, Tome III, Université de Batna, 1998.

[ABD 06] **Abelhak. ABDOU**, "Contrôle non destructif par courant de Foucault; Etude et réalisation d'un capteur inductif", Mémoire de Magister, Spécialité électrotechnique, Option matériaux d'électrotechnique, Université de Batna, 2006.

[AKN 01] **P. Aknin, M. Bentoumi, F. Fessant, F. Raux,** "Chaîne d'instrumentation embarquée pour la détection temps réel de défauts de rails débouchant", Colloque interdisciplinaire instrumentation, C21'2001, CMAP, Paris, 2001.

[AUL 10] **AULET. Alina, EIRAS. José A, et NEGREIRA, Carlos,** "Modeling, design and characterization of limited diffraction ultrasonic transducers", Physics Procedia, vol. 3, 2010, p p. 577-583.

[BAC 09] **Bachir Maouche, Rezak Alkama, Mouloud Feliachi**, "Semi-analytical calculation of the impedance of a differential sensor for eddy current nondestructive testing", NDT & E International, Elsevier 42 (2009) 573– 580.

[BEN 06] **Nabil. BENHADDA**, "Modélisation des capteurs inductif par courant de Foucault", Mémoire de Magister, Spécialité électrotechnique, Option matériaux d'électrotechnique, Université de Batna, 2006.

[BER 98] **G. Berthiau, B. de Barmon,** "MESSINE, An Eddy Current Parametric Model for flaw characterization ", Review of Progress in Quantitative Non Destructive Evaluation, QNDE'98, (Snowbird Utah, USA, 1998).

[BUR 04] **Noël. BURAIS, Alain. NICOLAS**, "Modèles pour la simulation des END par courants de Foucault", Journées COFREND, Lyon, Oct 2004.

[BOU 96] **J.C. Bour, E. Zubiri, P. Vasseur, A. Billmat,** "Etude de la répartition des courants pulsés dans une configuration de contrôle non destructif ", J. Phys. III, Janvier 96, pp. 7-22.

[BEL 03] **Yamina BELKHIRI**, " Modélisation des phénomènes électromagnétiques et mécaniques couples par la méthode des volumes finis (CVM) ", mémoire de magister, Spécialité électrotechnique, Université de Batna, 2003.

[BLI 97] **Blitz. J**, "Electrical and magnetic methods of nondestructive testing", Chapman and Hall, page 39, 1997.

[CHE 07] **Ahmed CHERIET**, "Contribution à la modélisation tridimensionnelle par la méthode des volumes finis de dispositifs électromagnétiques", Thèse de Doctorat, Université de Biskra, 2007.

[CHE 09] **A. Cheriet, M. Feliachi, and S. M. Mimoune**, "3D movement simulation technique in FVM method application to eddy current nondestructive testing", The International Journal for Computation and Mathematics in Electrical and Electronic Engineering, vol. 28, no. 1, pp. 77–84, 2009.

[CHO 09] **Yahya CHOUA**, **Laurent SANTANDRÉA, Yann LE BIHAN, Claude MARCHAND**, "Modélisation de défauts de faible ouverture pour le CND par courants de Foucault", CNI'09, Colloque National sur l'Inductique, Laghouat, N° 97, Avril 2009.

[CRU 15] **Cruza, J. F., Perez, M., Moreno, J. M., & Fritsch**, "Real time fast ultrasound imaging technology and possible applications". Physics Procedia, vol. 63, 2015, pp. 79-84.

[DUM 96] **J. DUMONT-FILLON**, "Contrôle non destructif (CND)", technique de l'ingénieur R1400, 1996, pp. (1-42).

[DON 10] Thickness measurement using laser triangulation
< http://www.sensorsmag.com/components/thickness-measurements-using-laser-triangulation.>

[ELG 15] **I. N. El ghoul, A. Cheriet, S. Bensaid**, "Evaluation de l'épaisseur des plaques conductrices par la Méthode des Courants de Foucault", 4ème colloque que l'inductique CI'2015, Jijel, Algérie.

[GIL 88] **Gilles PEIX**, "Contrôle non destructif par courant de Foucault", I.N.S.A. de Lyon, 1988.

[GOM 10] **T. E. Gomez, A. lvarez-Arenas**, "Simultaneous determination of the ultrasound velocity and the thickness of solid plates from the analysis of thicknes resonances using air-coupled ultrasound", Ultrasonics, Vol. 50, No. 2, pp. 104 109, Feb2010.

[HEL 06] **B. Helifa, A. Oulhadj, A. Benbelghit, I.K. Lefkaier, F. Boubenider, D. Boutassouna**, "Detection and measurement of surface cracks in ferromagnetic materials using eddy current testing", NDT&E International, Elsevier, Vol. 39, Issue 1, March 2006, pp. 384-390.

[HEL 12] **Bachir HELIFA**, "Contribution à la simulation du CND par courants de Foucault en vue de la caractérisation des fissures débouchantes", Thèse de Doctorat, Université de Nantes, 2012.

[HUR 06] **Do Haeng Hur, Deok Hyun Lee, Myung Sik Choi, Un Chul Lee, Seon Jin Kim, Jung Ho Han**, "Discrimination method of through-wall cracks in steam generator tubes using eddy current signals", NDT&E International, Vol. 39, 2006, pp.361–366.

[HUR 10] **Do Haeng Hur, Myung Sik Choi, Deok Hyun Lee, Seon Jin Kim, Jung Ho Han**, "A case study on detection and sizing of defects in steam generator tubes using eddy current testing, Nuclear Engineering and Design", Vol. 240, 2010, pp. 204–208.

[HMG 09] **H. M. Geirinhas Ramos, O. Postolache, F. Corrêa Alegria, A. Lopes Ribeiro**,"Using the skin effect to estimate cracks depths in metallic structures", 12MTC 2009, International Instrumentation and Measurement Technology Conference, Singapore, May 2009.

[HOL 98] **J.-E. Holmström, "**Exposure values for a 300 kV halfwave X-ray unit using three X-ray films of different film classes", NDT & E International, Vol. 31, Issue 1, 1998, pp. 33- 41.

[HON 15] **Hongbo Wang, Wei Li, and Zhihua Feng**, "Noncontact Thickness Measurement of Metal Films Using Eddy-Current Sensors Immune to Distance Variation", IEEE Trans. Instrum. Meas, Vol. 64, Issue 9, 2015, pp.2557-2564.

[JAC 96] **Jacques ATTAL**, " Microscopie acoustique", technique de l'ingénieur R1402, 1996, pp. (1-10).

[KRA 11] **J. Kral, R. Smid, H. M. G. Ramos, and A. L. Ribeiro**, "Thickness measurement using transient eddy current techniques", in Proc. I2MTC, Shangai, China, May 2011, pp. 138–143.

[KHE 06] **Mohamed Lotfi KHENE**, " Modélisation des phénomènes électromagnétiques dans les structures a géométries complexes par adaptation de la méthode des volumes finis", mémoire de magister, Spécialité électrotechnique, Université de Batna, 2006.

[LAK 10] **A. Lakhdari, A. Cheriet, M. Felliachi**, "Modélisation d'un capteur différentiel de CND-CF par la méthode des volumes finis", CEE'10, 6th International conference en electrical engineering, Batna, MAT97, N° 58, pp. 492-495, Oct 2010.

[LAK 11] **Ala-Eddine LAKHDARI,** "Etude Et Modelisation De Capteurs En Cnd Par Courants De Foucault : Application A La Detection Des Fissures", Mémoire de magister, Spécialité électrotechnique, Université de Biskra, 2011.

[LUB 15] **Lubeigt, E, Mensah, S, Chaix, J F, Rakotonarivo, S, Gobillot G, Baqué F**,"Ultrasonic Imaging in Liquid Sodium: A Differential Method for DamagesDetection". Physics Procedia, vol. 70, 2015, pp. 550-553.

[MAI 04] **Franz Mairinger**, "Chapter 2 UV-, IR- and X-ray imaging, Comprehensive Analytical Chemistry", Elsevier, Vol. 42, 2004, pp. 15-71.

[MOH 07] **Mohamed K. Bencharif**, "Contrôle par Ressuage",Vinçotte International Algérie, Mai 2007.

[MHE 07] **M'hemed Rachek, Mouloud Feliachi**, "3-D movement simulation techniques using FE methods: Application to eddy current non-destructive testing", NDT & E International, Elsevier, Volume 40, Issue 1, pp 35-42, January 2007.

[MAR 11] **H. Marret, A. Bleuzen, A. Guérin, M.-A. Lauvin-Gaillard, D. Herbreteau, F. Patat, F. Tranquar**t,"Résultats préliminaires de la destruction des fibromes utérins par ultrasons focalisés contrôlée par résonance magnétique", Gynécologie Obstétrique & Fertilité, Vol. 39, Issue 1, January 2011, pp. 12-20.

[MAA 94] **MS. MAALEM**, "Electricité Magnétisme et courant alternatif", Tome III, Université des sciences et de la technologie Houari Boumediene, 1994.

[OUK 97] **L. Oukhellou, P. Aknin**, "Structure multicapteur originale a courants de Foucault pour la détection en voie de défauts de rail", COFREND,Congrès sur les essais non destructifs. Nantes**,** 1997.

[OUK 97] **Latifa OUKHELLOU**, "Paramétrisation et Classification de Signaux en Contrôle Non Destructif. Application à la Reconnaissance des Défauts de Rails par Courants de Foucault", Thèse de Doctorat, Université Paris XI Orsay, 1997.

[PAU 05] **Paul E. MIX**, "Introduction to nondestructive testing: a training guide", Wiley Interscience**,** 2nd edition, United States of America, 2005.

[PET 12] **Petter Norli, Det Norske Veritas, Høvik Norway**, " Air-coupled Thickness Measurements of Stainless Steel", Institute of Micro and Nano Systems Technology, Oct. 2012.

[PAT 80] **S. V. PATANKAR**, "Numerical heat transfer and fluid flow", Series in computational methods in mechanics and thermal sciences. Hemisphere publishing corporation, 1980.

[PIN 14] **E. Pinotti, E. Puppin**, "Simple lock-in technique for thickness measurement of Metallic plates", IEEE Transactions on Instrumentation and Measurement, Vol. 63, No. 2, pp. 479-484, Feb. 2014.

[RAV 09] **C. Ravat, Y. Le Bihan, P. Y. Joubert, C. Marchand, M. Woytasik, E. Dufour Gergam, J. Moulin, E. Martincic**, "Detection of small surface breaking cracks using a microcoil array eddy current sensor", CNI'09, Colloque National sur l'Inductique, Laghouat, N° 98, Avril 2009.

[RIB 12] **A. Lopes Ribeiro, H. Geirinhas Ramos, J. Couto Arez**, "Liftoff insensitive thickness measurement of aluminum plates using harmonic eddy current excitation and a GMR sensor", Measurement 45 (2012) 2246–2253.

[STA 92] **K. Stake, M. Tanaka, N. Shimizu**, "Three-dimensional analysis on eddy current testing for S/G tube", IEEE Transactions on magnetics, vol 28, N°2, March 1992.

[WIL 00] **William H. Hayat. Jr, John A. Buck**, "Engineering electromagnetics", 6th edition, McGraw-Hill, Atlanta, 2000.

[WAI 56] **D. Waidelich**, "Measurement of coating thickness by use of pulsed eddy currents", Materials Evaluation, Vol. 14, pp. 14–15, 1956.

[YIN 08] **W. Yin and A. J. Peyton**, "Thickness measurement of metallic plates with an electromagnetic sensor using phase signature analysis", IEEE Trans. Instrum. Meas., vol. 57, no. 8, pp. 1803–1807, Aug. 2008.

[You 08] **Young joo KIM, Bong young AHN and Seung-seok LEE**, "Thickness measurement of aluminum plates with a pulsed eddy current method", Modern Physics Letters B, Vol. 22, No. 11 (2008) 911−915.

[ZER 10] **S. Zerguini, B. Maouche, A. Amira, and M. Latreche**, "Modélisation du CND-CF : Application à un Dispositif de Capteur à Fonction Séparées", CEE'10, 6th International conference en electrical engineering, Batna, MAT68, N° 281, pp. 341-344, Oct 2010.

[ZAO 09] **A. ZAOUI, M. FELIACHI, M. ABDALLAH**, "Modélisation d'une matrice de capteurs a courants de Foucault", CNI'09, Colloque National sur l'Inductique, Laghouat, N° 44, Avril 2009.

[ZAI 12] **Houda ZAIDI,** "Méthodologies pour la modélisation des couches fines et du déplacement en contrôle non destructif par courants de Foucault : application aux capteurs souples", Thèse de Doctorat, Université de Paris-sud 11, 2012.

[ZOR 12] **Chiara ZORNI**, "Contrôle non destructif par courants de Foucault de milieux ferromagnétiques : de l'expérience au modèle d'interaction", Thèse de Doctorat, Université de Paris-sud 11, 2012.

Abstract

When an inductive sensor traversed by an AC current is approached to a metal part, variable electric currents, called eddy currents, appear in this part. These eddy currents, depending on their distribution in the part in question, produce a variation in the impedance of the sensor. Depending on the application, measuring and analyzing this impedance variation can be used to detect faults, electromagnetic characterization of the part or identify the geometrical properties of the part. Indeed, several characteristic quantities of the part which are at the origin of the variation of the impedance of the sensor. These quantities are the electrical conductivity of the part, its magnetic permeability and the dimensions of the part (thickness, etc.). It is known that the thickness measurement by eddy currents is limited to a certain characteristic thickness because of the penetration thickness; the intensity of the eddy currents decreases with the depth below the surface according to an exponential law. In this project, we propose a multi-sensor system with an eddy current dedicated to the measurement of thickness exceeding this characteristic thickness.

Key words: Thick metal plates, thickness measurement, FVM, NDE-EC, multi-sensors.

Résumé

Lorsqu'un capteur inductif parcouru par un courant AC est approché d'une pièce métallique, des courants électriques variables, appelés courants de Foucault apparaissent dans cette pièce. Ces courants de Foucault, selon leur répartition dans la pièce en question, produisent une variation de l'impédance du capteur. En fonction de l'application, la mesure et l'analyse de cette variation d'impédance permet par la suite la détection des défauts, la caractérisation électromagnétique de la pièce ou l'identification des propriétés géométriques de cette pièce. En effet, plusieurs grandeurs caractéristiques de la pièce qui sont à l'origine de la variation de l'impédance du capteur. Ces grandeurs sont la conductivité électrique de la pièce, sa perméabilité magnétique et les dimensions de la pièce (épaisseur,…etc.). On sait que la mesure d'épaisseur par courants de Foucault est limitée à certaine épaisseur caractéristique à cause de l'épaisseur de pénétration ; l'intensité des courants de Foucault diminue avec la profondeur en dessous de la surface selon une loi exponentielle. Dans ce projet, on propose un système multi-capteurs à courant de Foucault dédié à la mesure d'épaisseur dépassant cette épaisseur caractéristique.

Mots clés : Plaques métalliques épaisses, mesure d'épaisseur, MVF, END-CF, multi-capteurs.

ملخص

عندما يولد المستشعر الحثي تيار متناوب ونقربه من لوحة معدنية تتولد تيارات تسمى بتيارات فوكو (التيارات الدوامة)،هذه الأخيرة تتوزع في المادة الناقلة مما ينتج عنه تغير في ممانعة المستشعر .اعتمادا على هذا التغير في الممانعة نستطيع أن نكشف عن الخلل الموجود في المادة و معرفة خصائصها الكهرومغناطيسية وتحديد خصائصها الهندسية. في الحقيقة العديد من القيم المميزة للمادة يمكننا معرفتها من خلال التغير في ممانعة المستشعر وهي : الناقلية الكهربائية، النفاذية المغناطيسية كما يمكننا معرفة أبعاد المادة (سمك ...الخ). من المعروف أن قياس السمك عن طريق تيارات فوكو محدود فهو يقتصر على خصائص السمك المراد قياسه وذلك بسبب سمك الاختراق، لأن شدة تيارات فوكو تتناقص كلما زاد اختراق المادة حسب القانون الأسي، في عملنا هذا نقترح طريقة لكيفية قياس سمك الألواح المعدنية السميكة عن طريق نظام متعدد المستشعرات بتيارات فوكو.

الكلمات المفتاحية : لوحة معدنية سميكة، قياس السمك ، طريقة الحجوم المنتهية، التقييم الغير هدام للمادة عن طريق تيارات فوكو، متعدد المستشعرات